Systematic study of the structure of odd-mass lanthanum nuclei. III. Levels in ^{133}La from the decay of 5-h ^{133}Ce

E. A. Henry and R. A. Meyer
Lawrence Livermore Laboratory, University of California, Livermore, California 94550
(Received 22 May 1978)

Levels of ^{133}La populated by the β decay of the $9/2^-$ 5-h isomer of ^{133}Ce were studied by γ-ray spectroscopy, γ-γ coincidence counting, and conversion-electron spectroscopy of mass-separated ^{133}Ce sources. The ^{133}La level scheme was greatly extended and substantial differences from previous level schemes were found. Both the observed negative and positive parity levels are accounted for in terms of decoupled band structure by calculations based on thee particle-plus-triaxial-rotor model. Deviations of this simple picture from the experimental data are discussed.

[RADIOACTIVITY ^{133}Ce [from Ba(α,Xn)]; measured $E\gamma$, $I\gamma$, I_{ce}, γ-γ coin; deduced log ft. ^{133}La deduced levels, J, π, ICC. Mass separation, chemical purification from ^{133}La.]

I. INTRODUCTION

In an attempt to gain a better understanding of the nature of transitional nuclei, we have undertaken a systematic study of the odd-mass La nuclei.[1,2] Our earlier work on ^{135}La and ^{137}La revealed the ability of the weak-coupling model to explain the behavior of these isotopes. However, this model fails for ^{133}La.[1,2] In this present work, we establish a detailed knowledge of the low energy excitations of ^{133}La. We then test the current models against our data, showing that the dressed n-quasiparticle formalism fails to account for all the ^{133}La levels and their properties. Finally, we show that the *total* low energy structure of ^{133}La can be accounted for, via triaxial model calculations, by requiring that all low energy excitations arise from decoupled bands built on the $g_{7/2}$ proton hole, the $d_{5/2}$ proton particle, and the $h_{11/2}$ proton particle excitations. The one failing of this picture appears when we attempt to account for a $\frac{1}{2}^+$ level that is observed at 173 keV but is predicted at approximately 400 keV. However, if the model is extended to include configuration mixing, resulting from coupling of the $d_{5/2}$ particle to the 2_1^+ core level (e.g., $\frac{1}{2}^+ | d_{5/2} 2_1^+\rangle$) with the $s_{1/2}$ single-particle state through a nonspin-flip matrix element, the energy of this $\frac{1}{2}^+$ level could be lowered significantly. We have discussed our initial results elsewhere.[3,4]

The last detailed studies of the decay of 5-h ^{133}Ce were those of Abou-Leila *et al.*[5] and Gerschel *et al.*[6,7] from which a level scheme for ^{133}La was deduced and J^π values were determined. The authors of these works concluded that the 535-keV level was probably a $\frac{3}{2}^-$ shape isomer and that the ^{133}La core had an oblate deformation. However, this interpretation was shown to be incorrect by Leigh *et al.*[8] Additionally, Ba(α, t) reaction studies by Nakai *et al.*[9] support a J^π assignment of $\frac{11}{2}^-$ for the 535-keV level.

In a series of related works, Stephens *et al.*,[10,11] Leigh *et al.*,[8] and Nakai *et al.*[9] reported on studies of the single-particle states and high spin, negative parity levels in odd-mass La nuclei and interpreted their results in terms of the odd particle coupled to a symmetric rotating core with a small prolate deformation. Recently, Chiba *et al.*[12] have reported on an in-beam γ-ray study in which positive parity yrast levels were observed. In addition, they observed two negative parity levels which they proposed were unfavored $\frac{9}{2}^-$ and $\frac{13}{2}^-$ members of the $h_{11/2}$ negative parity band. The interpretation of the high spin levels of ^{133}La also has been discussed by Deleplanque *et al.*[13] Meyer-ter-Vehn[14] and Toki and Faessler[15] have extended the particle-plus-rotating-core model to include a triaxial core shape and have made calculations for levels in ^{133}La. For the lighter mass ^{129}La and ^{131}La, Butler *et al.*[16] have shown that the values of the reduced transition probabilities in the $h_{11/2}$ yrast band can be understood with this triaxial model.

Additional measurements on ^{133}Ce and its decay have included conversion-electron measurements (Abdumalikov *et al.*[17] and Abdul-Malek and Naumann[18]), level lifetime measurements (Abou-Leila *et al.*,[5] Babadzhanov *et al.*,[19] Berg *et al.*,[20] and Morosov *et al.*[22]), and determination of the spins of the 97-min and 5-h ^{133}Ce isomers and the ^{133}La ground state.[23] Three determinations of the half-life of the long-lived isomer also have been made.[7,24,25] Measurements of the quadrupole moment of the 535-keV level have been undertaken[26-28]; however, the results have been incon-

sistent with each other and with other data. Most of these data are summarized in the *Nuclear Data Sheets* for $A = 133$.[29]

II. EXPERIMENTAL PROCEDURE

The production of ^{133}Ce sources necessarily leads to the production of the daughter activity ^{133}La, on which we have previously reported.[30] Many of the details of the experimental procedures are described in that work and in Refs. 1–4, including source production, chemistry, mass separation, γ-ray spectroscopy, γ-γ coincidence experiments, and data reduction.

The ^{133}Ce radioactivity was produced by the Ba(α, xn) reaction at the Lawrence Berkeley Laboratory 88-inch Cyclotron. The targets were transported to the Lawrence Livermore Laboratory where the cerium was chemically separated from the target material. The Ce fraction was mass-separated onto thin Al foil. These sources then were counted with large volume Ge(Li) detectors, low energy photon spectrometers, and a Compton suppression Ge(Li) system. The efficiency and linearity of these systems are routinely calibrated. Energy calibration of the ^{133}Ce lines was made by counting sources simultaneously with ^{182}Ta, ^{56}Co, ^{110}Ag^{m}, and ^{133}Sn as well as with ^{133}Ba which is produced by the source. The γ-ray singles spectra were analyzed with the computer code GAMANAL.[31] A La-Ce separation was performed on one source after mass separation; both fractions were counted so that positive assignment of γ rays to the parent and daughter could be made.

In additon to these studies, a portion of the Ba target material with Ce activity was counted immediately upon receipt (approximately 2.5 h after the end of irradiation) to observe the decay of the 97-min ^{133}Ce isomer. Neither chemistry nor mass separation was performed on this portion of the source. Sources on which chemistry and mass separation had been performed were available for counting approximately 8 h after the end of irradiation; virtually no activity due to direct production of this short-lived ^{133}Ce isomer was observed.

Internal conversion-electron measurements were performed using a spectrometer with a trochoidal magnet[32] which transports the electrons from the source to the detector in a magnetic field. Mass-separated sources deposited on a thin Al foil were used for the conversion-electron spectrometry. We used a 4-mm-thick Si(Li) detector with a full width at half maximum (FWHM) of 2.5 keV at 400 keV. Two conversion-electron spectra were taken. For electrons in the range of 200 to 700 keV, a magnet current of 40 A was used; a magnet current of 100 A was used for electrons in the range of 400 to 2000 keV. A useful data overlap occurred between 400 and 700 keV in these two runs, allowing a check of the normalization and uncertainties. The calibration sources used were ^{137}Cs, ^{139}Ce, ^{207}Bi, and ^{113}Sn. The overall absolute uncertainty in the intensity determination for these sources was 10%; however, the relative uncertainties were taken to vary from 3% near the normalization points to greater than 10% where no calibration points existed. A straight line constant extrapolation in the region above 1 MeV gave reasonable results in terms of transition multipolarity.

For γ-γ coincidence counting, we used the megachannel coincidence system,[33] which both accumulates the data and sorts the data during accumulation. Coincidences from a mixed source of ^{133}Ce and ^{133}La were detected with two 30-cm^2 Ge(Li) detectors in a 90° configuration. A standard slow-fast coincidence system with a 100-ns timing window was used. By setting a second timing window below the timing peak, we automatically corrected for chance coincidences. The total coincidence rate of approximately 150 coincidences per second had a true-to-chance ratio of approximately 12 to 1. Coincidence gates and nearby background gates (3 to 6 keV wide) were set on the gate spectrum. The resulting coincidence spectrum, with the background subtracted, was analyzed with GAMANAL to obtain coincidence peaks and then scanned visually to find weak coincidences of interest.

III. DATA AND RESULTS

The ^{133}La level scheme we propose differs substantially from that deduced by Gerschel.[6,7] Even for some levels at the same energy in these two schemes (e.g., 654 keV), the depopulation of the levels is very different. The spins and parities which we deduce are almost completely different from those proposed by Gerschel. Our level scheme also differs greatly from that proposed by Chiba *et al.*[12] Notably, we do not observe the $\frac{9}{2}^-$ level at 1313 keV or the $\frac{13}{2}^-$ level at 1294 keV as proposed by Chiba *et al.* The characteristics of the level that we tentatively suggest at 1188 keV are consistent with a $\frac{13}{2}^+$ assignment which also is indicated by Chiba *et al.* However, they place the 178-keV transition between the 654- and 477-keV levels, whereas our data show that this transition must be placed elsewhere in the level scheme.

The decay of ^{133}Ce results in a very complex γ-ray spectrum which includes the parent, daughter, and granddaughter decays. Figure 1 shows a portion of the γ-ray spectrum from 390 to 520 keV, taken with the Compton suppression Ge(Li) detector. In all, approximately 290 γ rays are assigned to 5-h ^{133}Ce decay and 5 γ rays are assigned to 97-

min ^{133}Ce decay. The γ-ray energies, relative intensities, and placements are summarized in Table I.

The ^{133}Ce conversion-electron spectrum taken at a magnet current of 100 A is shown in Fig. 2. Because the background is rapidly decreasing and the detector efficiency remains constant, useful conversion-electron data were obtained up to nearly 2 MeV. The conversion-electron data are summarized in Table II, along with the deduced conversion coefficients and transition multipolarities.

The conversion coefficients are normalized to $\alpha_k(477\gamma) = 0.009\,82$, the conversion coefficient for an $E2$ γ ray. In the conversion-electron data, the intensity due to the 475-keV γ ray cannot be meaningfully separated from that of the 477-keV γ ray; thus the 477-keV + 475-keV photon intensity is used in the normalization. The resulting normalization could be as much as 3.4% uncertain if the 475-keV γ ray is pure $M1$. This uncertainty is included in the calculated conversion coefficients. Multipolarities are determined by comparing the deduced conversion coefficients with the theoretical calculations of Hager and Seltzer[34] and Trusov.[35]

The efficiency of the conversion-electron detector system is not known accurately above 1 MeV. However, an internal check using the ^{133}Ce data indicates that the assumed constant efficiency probably is acceptable. The 1912-keV level has a 1377-keV γ ray to the $\frac{11}{2}^-$ 535-keV level, as well as a 1782-keV γ ray to the $\frac{7}{2}^+$ 130-keV level. The 2036-keV level has a 1494-keV γ ray to the $\frac{7}{2}^+(\frac{5}{2}^+)$ 541-keV level plus a 1500-keV γ ray to the $\frac{11}{2}^-$ 535-keV level. The deduced conversion coefficients of the 1377- and 1782-keV γ rays are consistent with $E2(+M1)$ and $E1$ multipolarities, respectively.

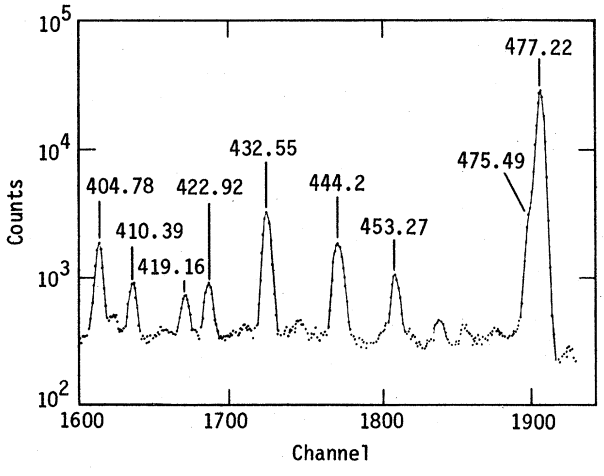

FIG. 1. A portion of the γ-ray singles spectrum from 400 to 480 keV taken with a Compton-suppression spectrometer.

Likewise, the conversion coefficients of the 1494- and 1500-keV γ rays are consistent with $E1$ and $E2(+M1)$ multipolarities, respectively.

The γ-γ coincidence results are summarized in Table III. Approximately 125 gates were set which resulted in useful coincidence relationships. The ^{133}La level scheme we have deduced for the 5-h ^{133}Ce decay is shown in Fig. 3. Energy sums and coincidence data were used to establish 55 definite levels and 8 tentative levels. One additional level is based on the decay of 97-min ^{133}Ce (Fig. 4). Approximately 98% of the photon intensity assigned to ^{133}Ce is placed in the proposed level scheme. The absolute photon-plus-conversion-electron intensities are given on the level scheme drawings.

We obtain the ^{133}Ce fractional β-decay intensities by summing the intensity of the transitions to the ground state. The multipolarities of the 87- and 130-keV γ rays are taken from Gerschel *et al.*,[6,7] whereas the 97-keV γ ray is assumed to be $M1$ for normalization purposes. The β decay to the ground state is assumed to be zero. Multiplying our relative γ-ray intensities by the factor 0.0387 ± 0.0012 gives the intensity per 100 decays of ^{133}Ce (assuming the relative intensity of the 477-keV γ ray is set at 1000). Decay directly to the ground state must be a first-forbidden unique transition

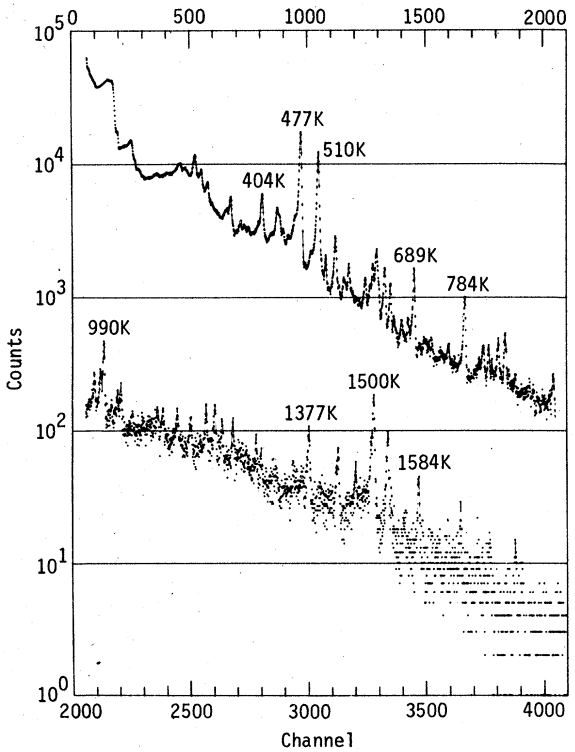

FIG. 2. The ^{133}Ce conversion electron spectrum from 0 to 2 MeV taken with the trochioidal spectrometer system using a Si(Li) detector.

TABLE I. Summary of the γ-ray energies (in keV), relative intensities, and placements of γ rays following ^{133}Ce decay. The γ rays of uncertain assignment are indicated by a question mark.

E_γ (ΔE_γ)	I_γ (ΔI_γ)[a]	Placement From	Placement To	E_γ (ΔE_γ)	I_γ (ΔI_γ)[a]	Placement From	Placement To
42.7 (1)?	2.0 (3)	130	87?	444.2 (1)	~35 } 59 (2)[e]	541	97
58.39 (3)	491 (10)	535	477		~24 }	980	535
76.9 (5)	350 (50)	174	97	453.27 (5)	25.4 (9)	541	97
87.939 (11)	131 (3)	87	0	455.28 (10)	2.8 (9)	950	495
97.261 (10)	44.8 (10)	97	0	460.5	~3.2 } 4.9 (6)[e]	1857	1396
97.261 (10)	1000 (150)	97	0		~1.7 }	591	130
130.803 (10)	457 (10)	130	0	475.49 (6)	81 (2)	563	87
173	<2.4	1153	980?	477.22 (4)	1000	477	0
174.0 (5)	9 (2)	174	0	495.07 (7)	15.4 (6)	495	0
174.0 (2)	1.6 (8)	1735	1561	498.72 (8)	5.1 (5)	1967	1468
177.3 (2)	1.3 (5)	654	477?	502.04 (9)	5.1 (12)	1690	1188
178.65 (3)	31 (1)	2036	1857	504.73 (8)	13 (3)	1045	541
204.16 (12)	1.3 (4)	...	...	510.36 (7)	528 (12)	1045	535
211.65 (6)	7.0 (5)	1365	1153	523.76 (5)	80 (2)	654	130
221.97 (9)	2.2 (4)	...	...	535	3 (1)	535	0
224.16 (7)	3.6 (4)	765	541	541.09 (10)	75 (10)	541	0
228.59 (6)	9.7 (5)	2035	1806	546.86 (8)	5.8 (5)	1735	1188
248.95 (2)	34.0 (8)	784	535	551.2 (2)	1.8 (5)	1092	541
256.6 (2)?	1.3 (5)	...	...	553.16 (15)	1.7 (5)	...	...
261.396 (14)	44.4 (10)	1045	784	557.7 (3)[b]	250 (50)	...	...
264.70 (10)	1.8 (4)	1310	1045?	560.09 (7)	15 (6)	...	...
274.84 (7)	3.4 (5)	838	563	566.5[c,d]	~1.7	2035	1468
278.0[d]	~6	2062	1784	571.06 (10)[d]	4.1 (10)	...	...
282.42 (5)	7.4 (5)	2036	1753	580.4	<1	1365	784
287.73 (8)	4.4 (6)	765	477?	581.12 (10)[d]	15.7 (15)	1561	980
294.23 (5)	12.7 (6)	1690	1396	591.24 (10)	5.5 (7)	591	0
300.54 (10)	6.1 (10)	2036	1735	597.36 (14)[d]	9.6 (8)	1092	495
307.30 (6)	23.8 (9)	784	477	602.5 (3)	5.9 (7)	1967	1365
315.45 (8)	5.1 (6)	1468	1153	611.83 (6)	66.2 (16)	1396	784
319.03 (7)	8.0 (7)	1365	1045	615.39 (12)	6.9 (8)	1092	477
320.72 (10)	3.4 (7)	2036	1715	617.7 (2)[d]	42 (6)	1153	535
339.03 (5)	24.9 (15)	1735	1396	621.8[d]	14 (6)	2018	1396
342.65 (9)	3.0 (5)	2200	1857	634.5 (2)	2.8 (10)	765	130
346.39 (5)	106 (2)	477	130	639.3 (2)	6.6 (10)	2036	1396
350.03 (11)	1.9 (4)	1188	838?	644.74 (4)	50.2 (12)	1690	1045
351	<2.3	1396	1045?	653.75 (12)[d]	11.2 (10)	784	130
360.96 (10)	2.4 (6)	838	477	656.47 (11)	3.3 (6)	1310	654
364.19 (4)	32.0 (8)	495	130	669.0 (2)	3.9 (5)	1857	1188?
369.9 (2)	4.8 (10)	...	...	678.3[d]	~7 } 21 (4)[e]	765	87
371.9 (3)	1.3 (4)	867	495		~14 }	1218	541
376.71 (9)	3.9 (5)	...	...	684.28 (8)	10.4 (8)	1468	784
376.7 (3)[b]	~20	...	...	689.48 (4)	105 (3)	1735	1045
380.7 (2)	1.9 (5)	1218	838?	692.36 (12)	2.6 (8)	...	...
384.6	<1.7	1365	980	697.19 (6)	9.8 (5)	2062	1365
389.37 (9)	5.4 (5)	477	87	699.58 (7)	6.2 (5)	1194	495?
392.16 (8)	8.1 (5)	...	...	702.37 (11)	3.1 (5)	1748	1045
397.75 (6)	15.3 (6)	495	97	707.41 (6)	10.1 (7)	838	130
404.78 (4)	43.3 (9)	535	130	711.42 (7)	12.5 (7)	1188	477
407.10 (10)	6.3 (5)	495	87	736.32 (11)	4.1 (6)	867	130
408.0	~2.4[d]	1561	1153	739.0 (3)	2.0 (10)	1785	1045?
410.39 (10)	18.4 (6)	541	130	740.84 (12)	7.0 (8)	2137	1396
415.4	2.5 (6)	...	...	742.9 (2)	3.2 (8)	...	...
419.16 (5)	12.0 (6)	1784	1365	747.76 (13)	5.1 (7)	1310	563
422.92 (5)	18.1 (6)	1468	1045	754.25 (12)	10.8 (6)	1734	980
432.55 (4)	90 (2)	563	130	759.04 (13)	4.2 (7)	2155	1396
437.69 (7)	4.2 (5)	1092	654	765.19 (12)	6.7 (7)	765	0

TABLE I. (*Continued*)

E_γ (ΔE_γ)	I_γ (ΔI_γ)[a]	Placement From	Placement To	E_γ (ΔE_γ)	I_γ (ΔI_γ)[a]	Placement From	Placement To
769.9 (2)	2.9 (5)	867	97	1154.68 (10)	16.9 (9)	2200	1045
779.16 (14)	5.0 (8)	867	87	1168.76 (14)	4.5 (9)	2036	867
784.55 (8)	246 (6)	...	...	1172.05 (10)	15.1 (9)	1735	563
790.2 (2)	2.2 (6)	...	...	1174.1 (3)	3.8 (10)	1715	541
792.8 (2)	2.8 (7)	...	...	1180.1 (2)	3.0 (7)	1715	535?
798.59 (15)	3.4 (6)	2360	1561	1183.33 (9)	28.0 (9)	1967	784
802.1 (3)	4.2 (7)	1365	563	1187.1 (2)	3.6 (7)	1778	591?
805.4 (2)	3.9 (6)	1958	1153	1190.33 (10)	11.8 (7)	1753	563
811.2 (3)	7.6 (15)	1857	1045	1196.28 (11)	16.1 (10)	1850	654
819.47 (15)[d]	22.7 (12)	950	130	1199.9 (2)[d]	40 (3)	1735	535
829.42 (15)	25.7 (9)	1365	535	1207.04 (11)	15.6 (9)	1748	563
834.77 (15)	10.9 (6)	2200	1365	1212.9 (2)[d]	20 (2)	1690	477
838.1 (2)	3.7 (6)	838	0	1217.7 (3)	2.8 (7)	1753	535?
841.37 (14)	12.7 (7)	1318	477?	1221.2 (3)	6.2 (15)[e]	1784	563
844.19 (14)?	7.1 (7)	...	...	1225.4 (3)	1.8 (6)	2175	950
862.29 (13)	17.7 (6)	950	87	1233.64 (11)	12.8 (8)	2018	784
867.2	≈8.2 } 10.7 (7)[e]	867	0	1238.0 (2)	3.6 (7)	1715	477?
	≈2.5 }	1912	1045	1245.1 (2)	5.4 (10)	2029	784
877.13 (14)	9.3 (8)	...	...	1249.1 (3)	4.3 (6)	1785	535?
879.5 (2)	4.9 (7)	...	...	1251.68 (15)	8.5 (7)	2036	784
887.7 (2)[d]	6.2 (12)	1365	477	1258.2	~10 } 22.2 (10)[e]	1912	654
901.79 (15)	5.0 (7)	...	...		~12 }	1735	477
906.13 (11)	11.1 (7)	1690	784	1265.57 (15)	9.2 (8)	1396	130
914.8 (3)	3.4 (7)	1045	130	1270.95 (14)	9.5 (8)	1806	535
930.87 (12)	4.4 (11)	1715	784	1277.47 (10)	16.0 (11)	2062	784
943.70 (9)	14.6 (10)	2036	1092	1287.58 (7)	21.9 (8)	1850	563
950.99 (7)	32.5 (8)	1735	784	1294.07 (11)	7.6 (7)	1857	563
961.8 (4)	4 (1)	1092	130	1301.2 (3)	2.7 (7)	1778	477?
963.6 (4)	4 (1)	1748	784	1305.0 (2)	3.8 (8)	...	...
968.7[d]	~3[e]	2122	1153	1309.7 (2)	5.0 (10)	1850	541
972.34 (9)	24.9 (11)	2018	1045	1314.1 (2)	4.9 (10)	2360	1045
983.9 (2)	~1.5 } 20.7 (8)[e]	2137	1153	1316.1 (2)[d]	4.6 (15)	1857	541
	19.2 }	2029	1045	1333.21 (15)	5.9 (11)	...	...
990.13 (5)	75 (2)	2036	1045	1348.02 (12)	7.2 (7)	2501	1153
997.25 (11)	6.3 (6)	...	...	1352.9 (5)	1.2 (7)	2137	784?
1000.2 (3)	2.2 (6)	1785	784?	1362.41 (9)	15.4 (7)	1857	495
1004.49 (10)	9.0 (6)	1092	87	1365.8 (2)	2.9 (6)	...	...
1016.22 (9)	12.3 (6)	2062	1045	1369.9 (4)	1.2 (6)	2734	1365?
1019.24 (14)	3.0 (6)	...	...	1377.22 (7)	44 (1)	1912	535
1022.24 (12)	9.9 (8)	2175	1153	1380.19 (11)	6.4 (7)	1857	477
1036.3 (3)	3.1 (15)	1690	654	1395.1 (3)	2.2 (7)	1958	563
1066.3 (3)	2.2 (8)	1850	784	1404.51 (11)	5.4 (6)	1967	563
1073.20 (12)	7.3 (8)	1857	784	1407.5	1.2 (6)	2062	654?
1076.6 (2)	3.8 (7)	2122	1045	1419.9 (3)	3.0 (7)	1983	563
1081.1 (2)	6.6 (10)	1735	654	1423.1 (4)	1.1 (5)	1958	535
1085.43 (13)	12.0 (12)	1850	765	1432.22 (7)	30.6 (8)	1967	535
1091.7 (2)	~19 } 31 (2)[e]	2137	1045	1435.6 (3)	1.3 (6)	1912	477
	~12 }	1857	765	1447.7 (4)	0.8 (4)	1983	541?
1107.1 (3)	2.8 (7)	1194	87?	1455.3 (5)	~1.1 } 2.3 (6)[e]	2018	563
1109.44 (14)	4.9 (7)	2155	1045		~1.2 }	2501	1045
1121.5 (2)	2.5 (7)	1218	97	1465.3 (2)	~2 } 18.9 (8)[e]	2029	563
1128.0 (2)	6.0 (10)	1912	784		16.9 }	2249	784
1129.7 (2)	12.3 } 13.5 (10)[e]	2175	1045	1472.08 (11)	7.1 (8)	2035	563
	~1.2 }	1784	654	1494.85 (5)	82 (2)	2036	541
1135.9 (3)	1.7 (6)	2501	1365?	1498.9 (3)	7.4 (5)	2062	563
1143.0 (4)	1.3 (6)	2122	980?	1500.41 (6)	~2 } 123 (3)[e]	2155	654
1152.05 (11)	11.3 (8)	1806	654		121 (4) }	2036	535

TABLE I. (*Continued*)

E_γ (ΔE_γ)	I_γ (ΔI_γ)[a]	Placement From	Placement To	E_γ (ΔE_γ)	I_γ (ΔI_γ)[a]	Placement From	Placement To
1506.28 (12)	5.3 (7)	1983	477	1931.4 (2)	7.6 (11)	2062	130
1521.03 (10)	14.5 (9)	2062	541	1941.83 (15)	7.3 (6)	2029	87
1526.56 (6)	63 (2)	2062	535	1960.3 (5)	~1.8	2501	541
1544.47 (15)	3.1 (6)	...	...	1962.9 (3)	6.5 (10)	...	...
1557.82 (10)	9.2 (13)	2035	477	2001.9 (3)	1.8 (4)	2132	130
1567.9 (3)	1.9 (8)	...	...	2018.23 (11)	34.8 (8)	2018	0
1573.65 (10)	8.1 (6)	2137	563	2030.4 (3)	2.5 (4)	2029	0
1584.62 (6)	61 (2)	1715	130	2044.09 (7)	17.8 (6)	2132	87
1595.43 (11)	6.9 (6)	2249	654	2051.45 (12)	1.1 (2)	...	...
1601.3	~1.8	2137	535?	2057.4 (3)	0.4 (1)	...	...
1612.3 (2)	3.8 (6)	2175	563	2063.8 (3)	0.94 (10)	...	...
1620.0 (2)	4.6 (7)	2155	535	2069.2 (3)	0.66 (10)	2200	130
1623.0 (3)	2.4 (6)	1753	130	2075.0 (3)	0.65 (8)	...	...
1636.7 (2)	11.5 (6)	2200	563	2090.5 (3)	0.99 (10)	...	...
1640.2 (3)	3.7 (6)	2175	535	2095.8 (4)	0.49 (8)	2572	477?
1646.9 (3)	3.1 (8)	1778	130?	2111.84 (13)	15.2 (9)	2200	87
1653.4 (2)	12.3 (8)	1784	541	2119.2 (2)	32 (2)	2249	130
1658.9 (3)	4.3 (5)	2200	541	2132.1 (3)	1.0 (1)	2132	0
1664.4 (2)	19.2 (8)	2200	535	2147.2 (3)	2.2 (2)	...	...
1678.3 (3)[d]	6.6 (12)	2155	477	2160.0 (4)	0.90 (10)	...	...
1683.2 (3)	3.5 (5)	...	...	2167.6 (4)	0.94 (10)	2298	130?
1686.0 (4)	1.8 (5)	...	...	2186.1 (4)	1.9 (2)	...	...
1698.0 (3)	7.5 (6)	2851	1153	2196.4 (4)	0.38 (7)	2851	654
1705.5 (3)	4.2 (7)	2572	867?	2210.6 (4)	1.05 (8)	2298	87?
1712.4 (3)	3.2 (6)	2367	654	2217.1 (4)	0.40 (6)	...	...
1720.2 (2)	32.7 (8)	1850	130	2237.0 (5)	0.35 (7)	2367	130
1722.7 (3)	4.5 (7)	2200	477	2249.9 (8)	0.19 (5)	2250	0?
1726.7 (3)	5.0 (6)	1857	130	2279.1 (6)	1.3 (1)	2367	87
1769.36 (8)	31.1 (7)	1857	87	2291.2 (7)	0.41 (6)	...	...
1782.03 (7)	17.6 (8)	1912	130	2314.4 (8)	0.32 (5)	2851	535
1824.4 (4)	2.4 (8)	1912	87?	2320.1 (9)	0.72 (7)	...	...
1837.3 (3)	3.1 (7)	1967	130	2349.0 (10)	0.27 (4)	...	...
1846.5 (4)	1.1 (5)	2501	654	2367.6 (10)	0.20 (5)	2367	0
1852.3 (2)	14.0 (7)	1983	130	2373.6 (6)	0.48 (6)	2851	477
1858.0 (3)	2.0 (5)	1857	0?	2441.8 (11)	0.13 (5)	2572	130?
1872.4 (4)	0.8 (4)	2367	495?	2474.8 (11)	0.31 (7)	2572	97?
1876.3 (3)	2.6 (14)	...	...	2575.7 (4)	0.63 (6)	...	...
1887.3 (3)	25.9 (8)	2018	130	2604.0 (9)	0.30 (4)	2734	130?
1890.3 (3)	1.8 (7)	2367	477	2720.5 (10)	0.07 (3)	2851	130
1899.1 (2)	4.2 (6)	2029	130	2734.1 (11)	0.16 (3)	2734	0?
1905.1 (3)	1.7 (5)	2036	130	2863.4 (13)	0.10 (3)		

[a] Normalized to $I_{477\gamma}$ = 1000 for 5-h ^{133}Ce decay and $I_{97\gamma}$ = 1000 for 97-min ^{133}Ce decay.
[b] These γ rays are assigned to 97-min ^{133}Ce decay by their half-life.
[c] The γ ray is observed in coincidence data only.
[d] Interference from ^{133}La decay.
[e] Intensity determined or apportioned from coincidence data.

($\log f_1 t > 8.5$). The Q value, lifetime, and $\log ft$ value give a decay to the ground state of <18%. This adds less than 0.1 to the deduced $\log ft$ values for excited levels.

The $\log ft$ values are determined from the intensity balance at each excited level. The Q value is taken as a systematic value of 3300 keV (Ref. 36) and the half-life as 4.93 h.[25] The decay branches and $\log ft$ values are summarized on the level scheme drawings (Figs. 3 and 4). For levels below 2300 keV with well-known β branches, the uncertainty in the $\log ft$ values falls between 0.12 and 0.21, assuming there is no ground state β branch. Most of this uncertainty results from an assumed uncertainty of 200 keV in the Q value.

Only a total β branch to the 87-, 97-, and 130-

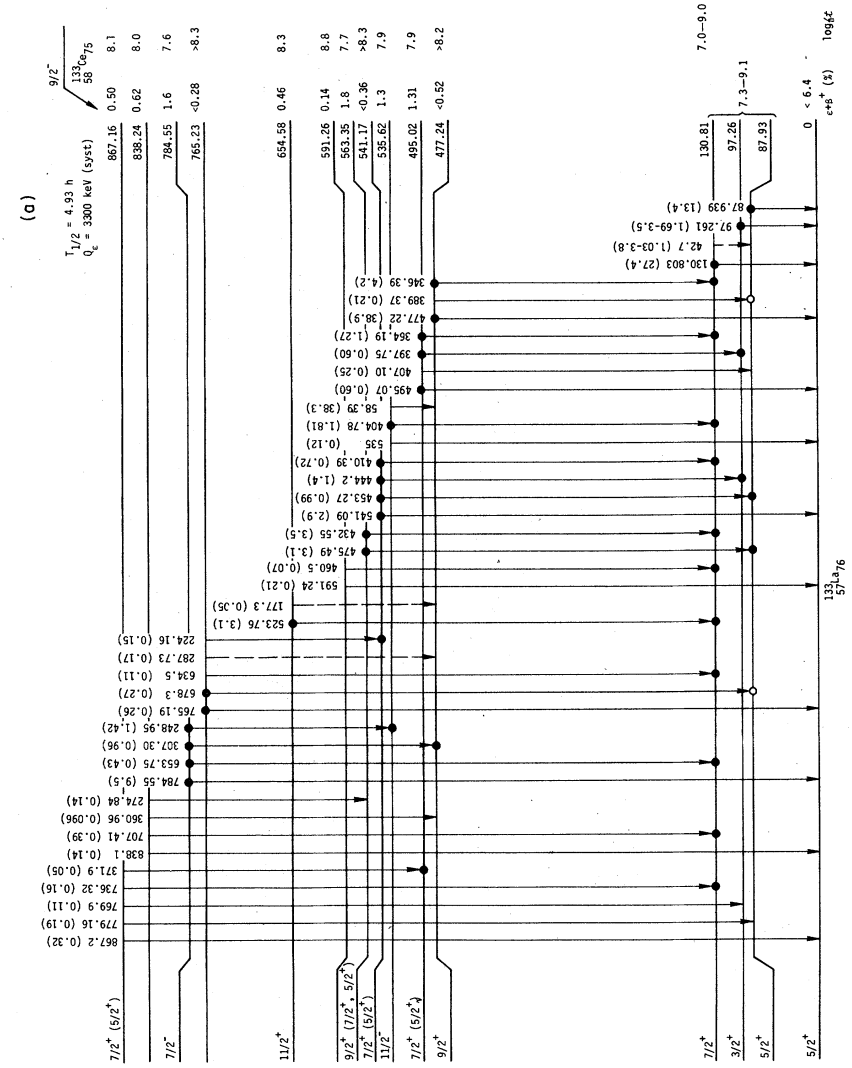

FIG. 3. The ^{133}La level scheme deduced from decay of ^{133}Ce.

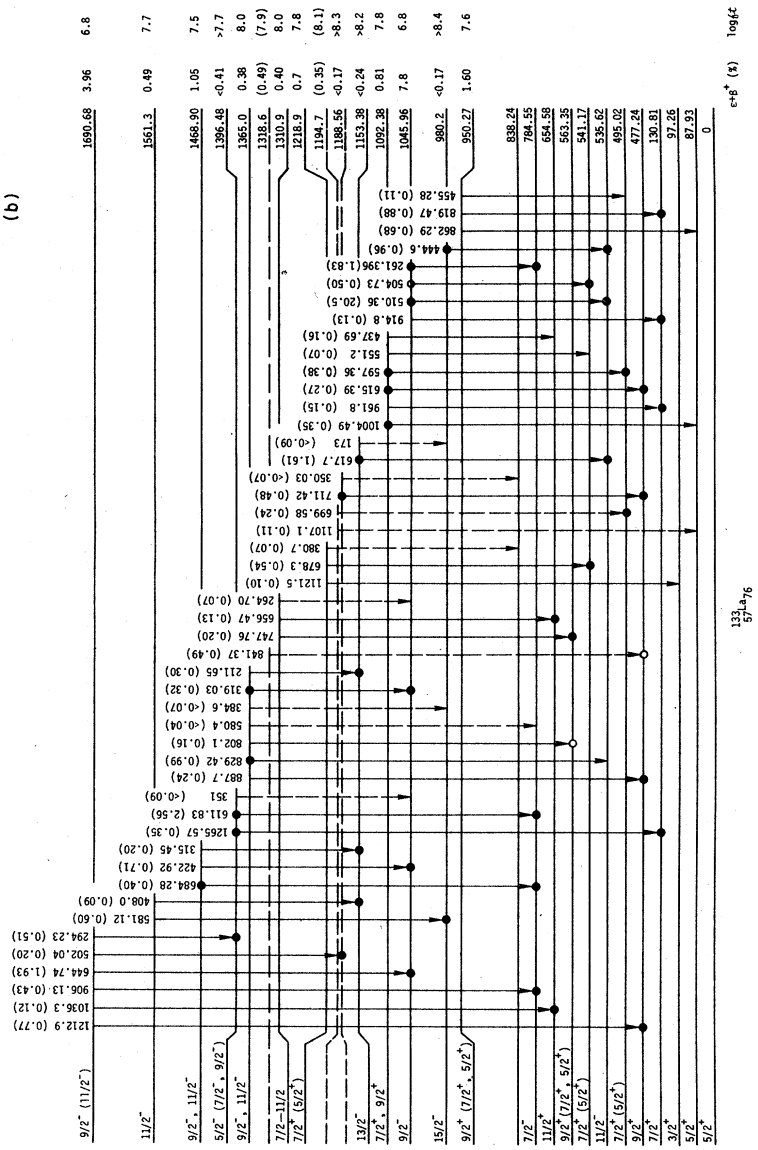

FIG. 3. (*Continued*).

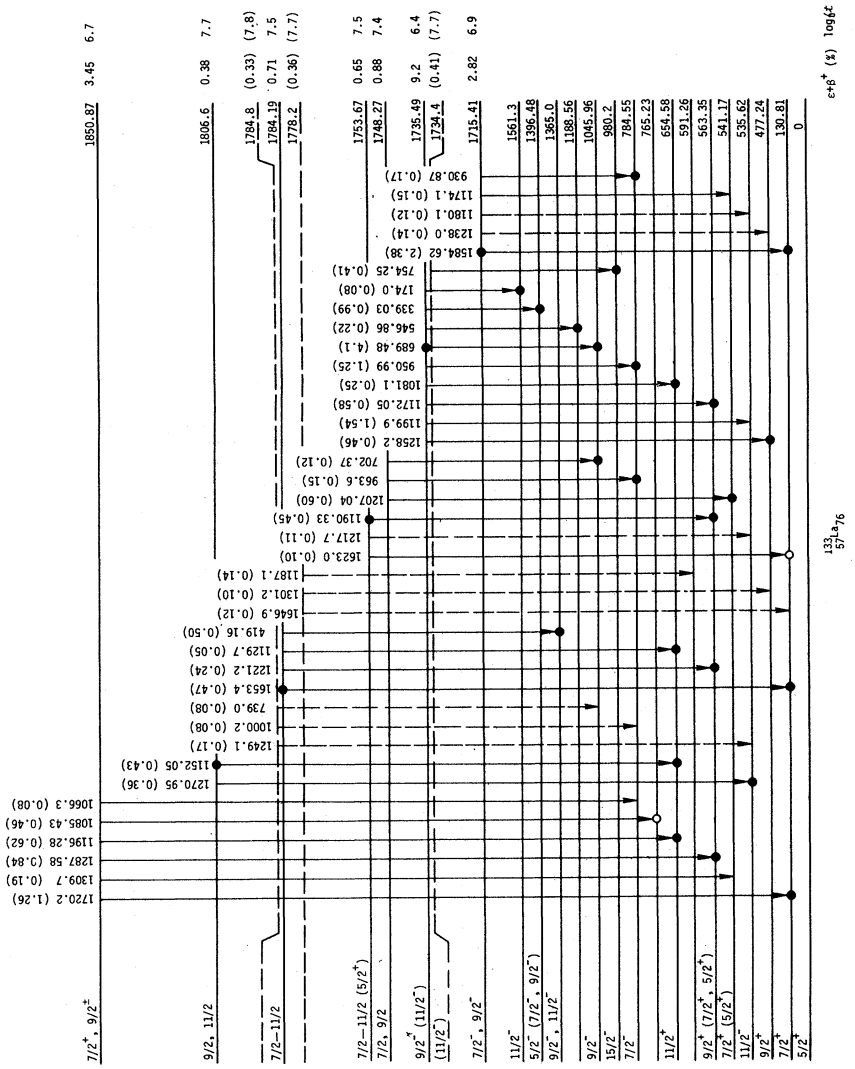

FIG. 3. (*Continued*).

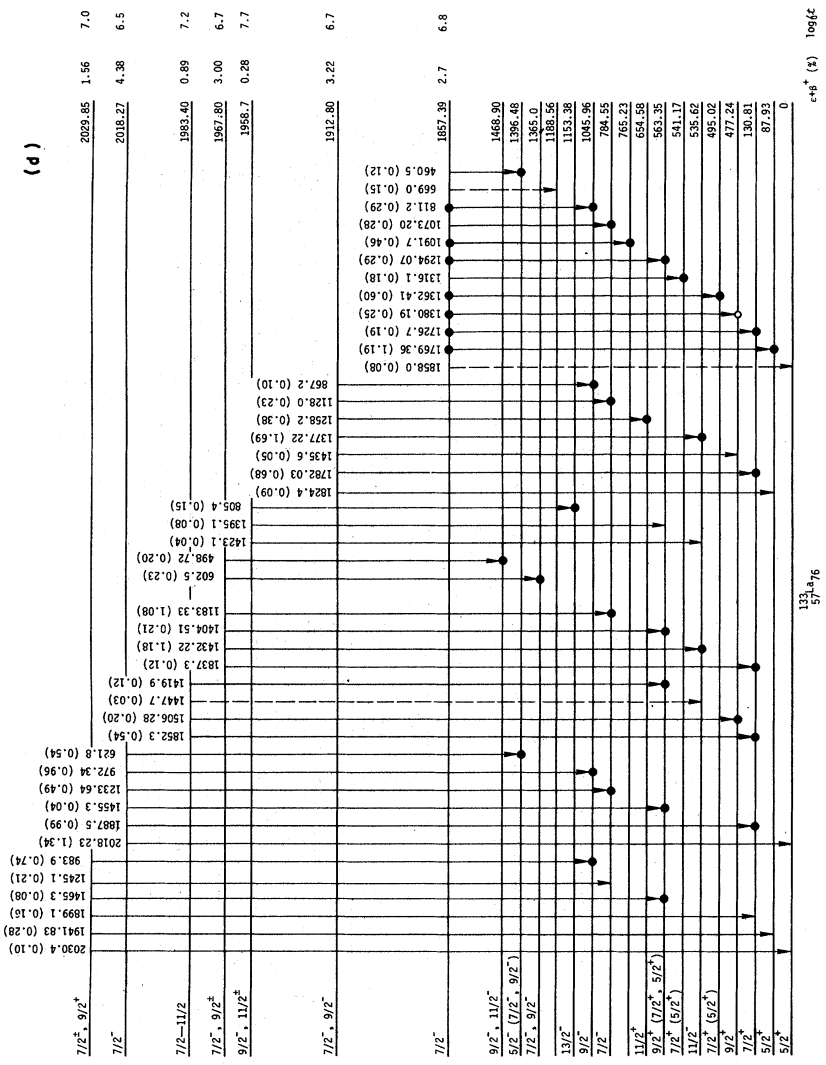

FIG. 3. (*Continued*).

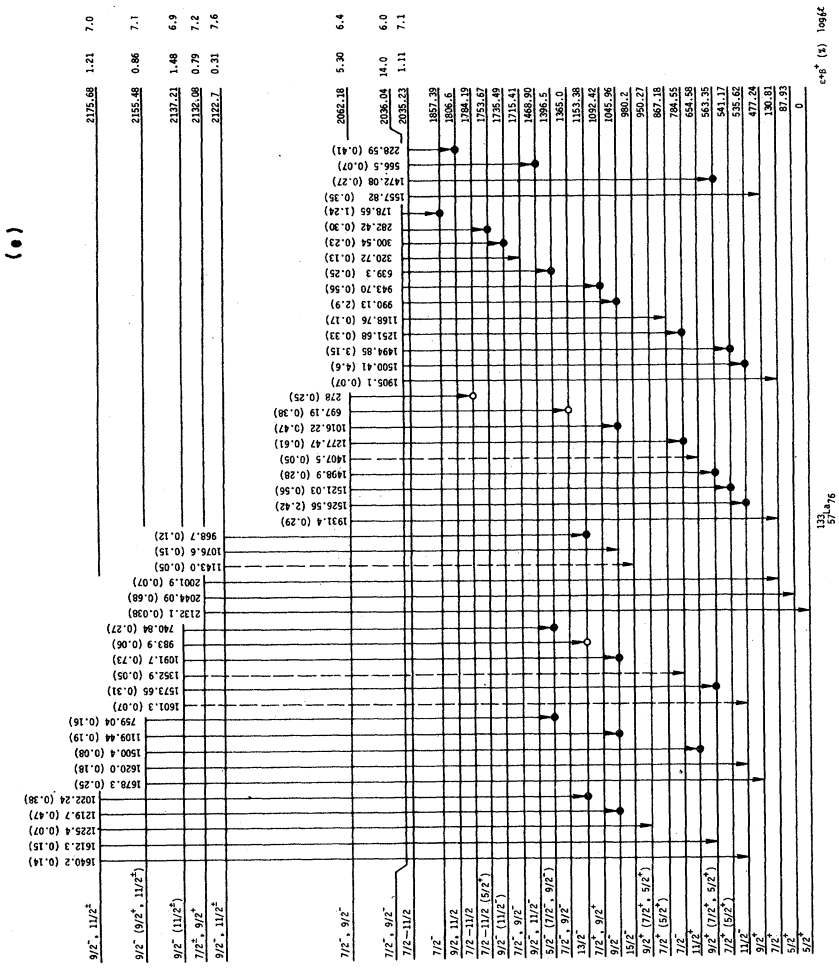

FIG. 3. (*Continued*).

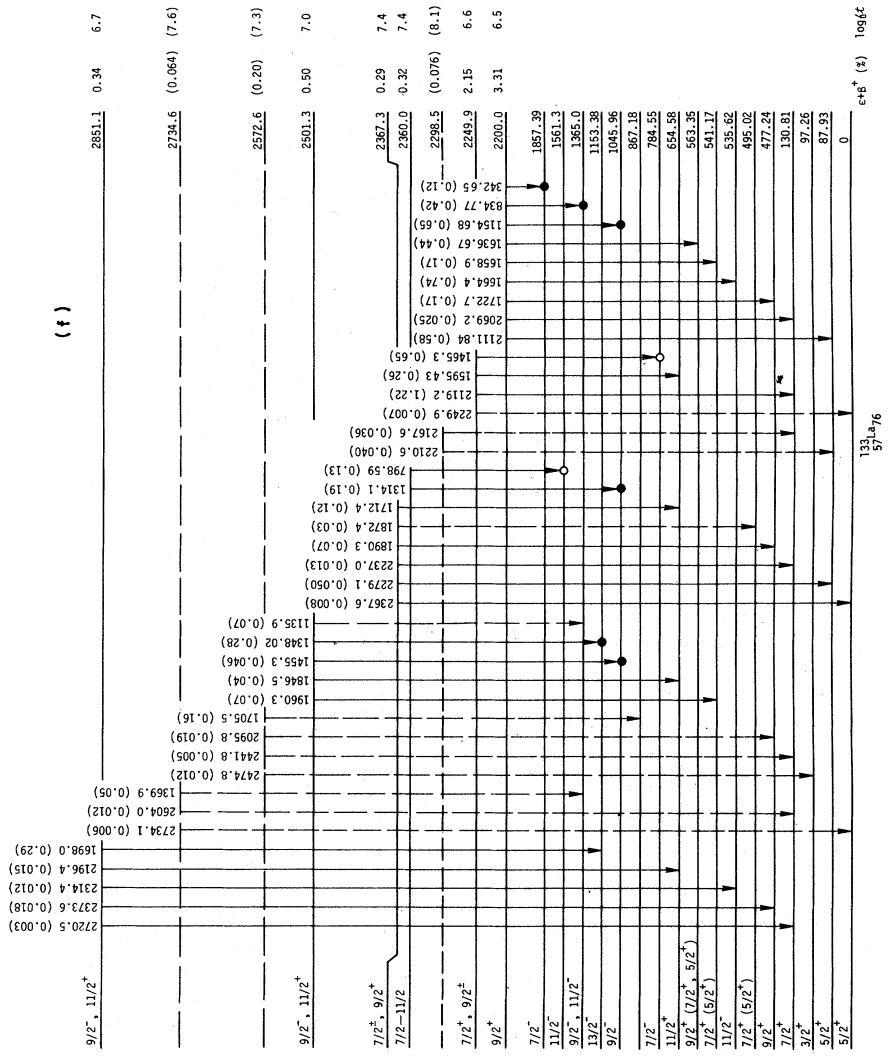

FIG. 3. (*Continued*).

TABLE II. The conversion-electron relative intensities as well as the deduced conversion coefficients and transition multipolarities for transitions in ^{133}Ce.

ID	E_{ce}	I_{ce} (ΔI_{ce})	I_γ (ΔI_γ)	α ($\Delta\alpha$)	Λ
346K	307	320 (70)	106 (2)	0.032 (8)	$M1, E2$
364K	325	68 (21)	32.0 (8)	0.023 (8)	$E2, M1$
404K	366	291 (35)	43.3 (9)	0.071 (3)	$M2$ + (<31%) $E3$
432K	393	94 (15)	90 (2)	0.011 (2)	$E2$ (+$M1$)
444K	404	58 (7)	59 (2)	...	...
453K	415	31 (5)	25.4 (9)	0.013 (3)	$E2$ (+$M1$)
475K + 477K	438	1000	1081	0.00982[a]	$E2$[a]
510K	471	643 (34)	528 (12)	0.0129 (9)	$M1$ + (<3%) $E2$
523K	485	47 (5)	80 (2)	0.0062 (7)	$E2$
542K + 510L	503	107 (8)	...	...	...
611K	573	45 (4)	66.2 (16)	0.0072 (8)	$M1$ + (±5%) $E2$
617K[b,c]	579	~25	42 (6)	0.0064	$M1$
644K	605	29 (4)	50.2 (12)	0.0061 (9)	$M1$ (+$E2$)
689K	650	61 (5)	105 (3)	0.0062 (6)	$M1$ (+$E2$)
784K	745	38 (3)	246 (6)	0.0016 (2)	$E1$ + (5 ± 3%) $M2$
819K	780	9.4 (10)	22.7 (12)	0.0044 (6)	$M1$ (+$E2$)
829K	790	7.5 (9)	25.7 (9)	0.0031 (4)	$M1$ (+$E2$)
834K	795	3.1 (7)	10.9 (6)	0.0030 (7)	$M1, E2$
906K	867	2.6 (5)	11.1 (7)	0.0025 (6)	$M1, E2$
950K	912	5.3 (7)	32.5 (8)	0.0017 (3)	$E2$ (+$M1$)
972K	933	6.1 (7)	24.9 (11)	0.0026 (4)	$M1$ (+$E2$)
990K	951	16.6 (16)	75 (2)	0.0023 (3)	$M1$ (+$E2$)
1016K	977	3.4 (5)	12.3 (6)	0.0029 (5)	($M1$)
1091K	1052	2.5 (5)	31.2	...	...
1128K + 1129K	1089	2.4 (5)	...	...	...
1151K + 1154K	1115	2.5 (5)	...	...	...
1183K	1144	3.3 (5)	28.0 (9)	0.0013 (3)	$E2, M1$
1199K[b]	1160	4.0 (6)	...	...	...
1212[b]	1173	2.1 (4)	...	...	...
1233K	1194	2.1 (4)	12.8 (8)	0.0017 (4)	$M1$ (+$E2$)
1277K	1237	1.2 (3)	16.0 (11)	0.0008 (3)	$E2$ (+$M1$)
1377K	1338	3.5 (5)	44 (1)	0.00084 (13)	$E2$ (+$M1$)
1432K	1392	2.4 (4)	30.6 (8)	0.00083 (15)	$E2$ (+$M1$)
1494K	1454	1.8 (4)	82 (2)	0.00023 (6)	$E1$
1500K	1460	7.8 (11)	121 (4)	0.00068 (11)	$E2$ (+$M1$)
1526K	1486	3.6 (8)	63 (2)	0.00061 (14)	$E2$ (+$M1$)
1584K	1544	1.5 (3)	61 (2)	0.00026 (6)	$E1$
1664K	1625	0.5 (2)	19.2 (8)	0.00028 (12)	$E1$
1769K	1730	0.60 (18)	31.3 (7)	0.00020 (7)	$E1$
1781K	1743	0.40 (16)	17.6 (8)	0.00024 (10)	$E1$

[a] Normalization.
[b] Interference from ^{133}La.
[c] Corrected for 615-keV γ ray from ^{133}Ce and 617-keV γ from ^{133}La.

keV levels can be deduced. A weak photon at 42 keV, which could feed the 87-keV level, is observed in spectra taken under favorable experimental conditions. The large difference between the $M1$ and $E2$ conversion coeffcients means that this transition, if present, could account for 20 to 90% of the observed feeding of the 87-keV level, with the remainder due to β feeding. The multipolarity of the 97-keV γ ray is $M1$ but could contain substantial $E2$; thus the feeding to the 97-keV level ranges from 1.7 to 3.5%. Because this is a low spin level, no direct β feeding from the high spin 5-h ^{133}Ce isomer can occur.

In addition, a 33-keV transition is possible from

TABLE III. Summary of the γ rays in coincidence with the gated γ ray.

Gate[a]	Coincident γ rays[b]
87	(389), 453, 475, (678), 1769
97	346, 397, 444, 1494
130	346, 364, 404, 410, 432, 460, 523, 634, 653, 707, 736, 819, 914, 1265, 1494, 1584, 1595, (1623), 1653, 1720, 1726, 1782, 1837, 1852, 1887
222 + 224	541, 1091
228	130, 528, 1152
248	261, 404, 477, 611, 906, (930), 950, 1183, 1233, 1251, 1277
261	248, 307, 644, 653, 689, 784, 811, 972, 983, 990, (1016), (1091), (1129), 1154
282	1190
294	248, 611, 784
300	689
307	130, 261, 346, 477, 930, 950
315	617
319	510, 834
339	248, 611, 784, 1265
346	130, 307, 510, 617, 1500, 1526
364	130, 371, 597, 699, 1362
389 + 392	(87)
397	597, 1362
404	130, 248, 444, 510, 617, 1500, 1526
410	130, 224, 1494
419	829
422	261, 477, 510
432	130, 747, 1172, 1190, 1221, 1287, 1294, 1404, 1419, (1465), 1472, 1498
444	97, 130, 504, 581, 754, 1207, 1494, 1521
453	87, 504, 1494
460	130
475 + 477	87, 178, 307, 510, 611, 615, 689, 711, (841), 887, 972, 983, 990, 1199, 1212, 1221, 1258, 1287, 1377, (1380), 1432, 1472, 1500, 1526
495	597, 699, 1362
504	410, 444, 453, 541, 689, 990
510	130, 319, 346, 404, 422, 477, 560, 644, 689, 702, 811, 867, 972, 983, 990, 1016, 1091, 1109, 1129, 1154, 1314, 1455
523	130, 656, 1036, 1081, 1129, 1152, 1196, 1258
541	504, 689, 1207, 1316
546	477, 711
567	422
581	174, 444, 617, (798)
611	130, 248, 294, 307, 339, 461, 477, 622, 639, 653, 740, 759, 784
617	211, 315, 408, 477, 805, 968, (984), 1022, 1348
621	611
644	261, 346, 404, 477, 510, 784
653	130, 261
678	(87), 444, 453, 541, 1091
684	498, 566, 784
689	261, 300, 346, 477, (504), 510, 784
697	(617)
699	130, 364, 397, 495
707	130
711	346, 477, 502, 546
736	130
740	611, 784
747	432, 475
754	444
759	611
784	261, 339, 611, 644, 684, 689, 906, 930, 950, 963, 990, 1073, 1128, 1183, 1233
802	(432), (475)
811	178, 510
829	419, 602, 834
834	829
867	510
906	248, 307, 784
930	784
943	364, 397, 495, 597, 615, 1004
950	248, 307, 653, 784
961 + 963	130, 784
972	261, 477, 510, 784
983	261, 510, 617
990	248, 261, 477, 510, 784
1016	261, 510
1022	617
1073	178, 784
1091	178, 510, 678, 765
1107 + 1109	477, 510
1128	(784)
1129	510, 523
1152 + 1154	130, 228, 477, 510, 523
1183	248, 307, 784
1190	130, 282, 432, 475
1196	130, 523
1199	477
1207	444, 541
1212	477
1221	432, 475
1233	248, 307, 784
1251	248, 477
1258	346, 477, 523, 617
1265	130, 339
1270	477
1287	130, 432, 475
1294	130, 178, 432, 475
1314 + 1316	510, (541)
1362	130, 178, 364, 397, 495
1377	477
1380	178, (477)
1404	432, 475
1419	130, 432, 475
1432	477
1455	432, 475, 510
1465	(248), 432, 475
1472	432, (475)
1494	130, 410, 444, 453
1498	130, 432, 475
1500	130, 346, 404, 477, 523
1506	346, 477
1521	444, (453)
1526	346, 477

TABLE III. (*Continued*)

Gate[a]	Coincident γ rays[b]
1573	130, 432
1584	130
1595	130
1620 + 1623	(130)
1636	130
1653	(278)
1720 + 1722	130
1769	87
1782	130
1852	130
1887	130

[a] Gates were 4 to 8 keV wide, centered on the γ ray of interest.
[b] The γ rays in parentheses appeared weakly in coincidence gates or were interfered with by other γ rays and thus are tentative.

the 130-keV level but is unobservable because of the presence of x rays at that energy. However, a coincidence between the 97-keV γ ray and the 346-keV γ ray which feeds the 130-keV level points to the existence of this transition. The possibility exists that a weak isomeric transition from the 5-h ^{133}Ce could make a very small contribution to the feeding of the 97-keV level. As a result of these uncertainties, the β feeding to the 130-keV level cannot be accurately determined; only a range of logft values can be deduced. Decay of the 97-min isomer of ^{133}Ce is only incompletely known (see Fig. 4). If we assume that the 97.26- and 76.9-keV transitions have $M1$ multipolarity and if we ignore the placement of the 577-keV γ ray, a crude estimate can be made that about 50% of the decays go to each of the 97- and 174-keV levels.

The spins (or limits on the spins) and the parities of most of the excited states of ^{133}La are determined by this experiment. The ground state of ^{133}La is $\frac{5}{2}^+$ (Ref. 23), the spin of the 5-h isomer of ^{133}Ce is measured to be $\frac{9}{2}$, and the spin of the 97-min isomer is $\frac{1}{2}$. On the basis of the available Nilsson states and systematics, the parities of the two ^{133}Ce isomers are minus and plus, respectively. The spins and parities of the 130-, 477-, and 535-keV levels are established to be $\frac{7}{2}^+$, $\frac{9}{2}^+$, and $\frac{11}{2}^-$, respectively, from the conversion-electron data of Gerschel[6] and the reaction results of Nakai *et al.*[9]

The $M1$ multipolarity of the 87-keV γ ray and a transition from the $\frac{9}{2}^+$ 477-keV level effectively limit J^π to $\frac{5}{2}^+$ or $\frac{7}{2}^+$ for the 87-keV level. On the basis of systematics, we assign this level to $\frac{5}{2}^+$. The 97-keV level is fed through the decay of both the high spin and low spin ^{133}Ce isomers. From conversion-electron data,[17] the 97-keV transition is found to be largely $M1$. There is no transition to this level from the $\frac{9}{2}^+$ 477-keV level. With this evidence, we assign the 97-keV level a J^π of $\frac{3}{2}^+$.

The transitions that depopulate the 174-keV level have no observable long-lived component. This level is fed by the $\frac{1}{2}^+$ isomer and has transitions to the $\frac{3}{2}^+$ 97-keV level and to the $\frac{5}{2}^+$ ground state. On the basis of these data and systematics, we assign the 174-keV level a J^π of $\frac{1}{2}^+$.

The spin and parity assignments to other excited levels in ^{133}La are summarized in Table IV. These assignments are based on logft values, deduced conversion coefficients, (HI, $xn\gamma$) reaction studies, and the assumption that the transitions for which we do not have conversion coefficients are $E1$, $M1$, or $E2$ multipolarity. For all levels below 1600 keV, except the 1045-keV level, first-forbidden unique β feeding is possible. However, above 1600 keV, first-forbidden unique β decay is possible only to definitely established levels at 1748, 1753, 1784, 1806, 1958, and 2122 keV.

IV. DISCUSSION

It has not been possible previously to account for the density and properties of the low energy levels in ^{133}La. In this discussion, we first examine the negative parity levels and show how all their properties can be accounted for up to approximately 2 MeV. Next, we discuss the positive parity levels and the difficulty encountered when trying to account for their properties with a "dressed" n-quasiparticle model. We then extend the concept of decoupling to the positive parity levels in an attempt to account for all observed levels up to approximately 1.5 MeV

A. Negative parity levels

We have discussed some details of the negative parity levels previously.[3,4] We have shown that the particle-plus-triaxial-rotor model can reproduce both the level energies and the ratios of transition rates of the levels built upon the $h_{11/2}$ single-particle state at 535 keV. We extend these discussions and include a more detailed comparison with the symmetric rotor case ($\gamma = 0°$). This comparison is important because the value of γ cannot always be extracted from the level energies of the core nuclei. Such a case is ^{105}Pd which is best fitted with a symmetric rotor calculation,[37,38] even though $\gamma \approx 24°$ is extracted from the level energies of ^{104}Pd and ^{106}Pd.

Shown in Fig. 5 are the experimental negative parity levels in ^{133}La up to approximately 1750 keV and the levels from two calculations using particle-plus-triaxial-rotor code, written by J. Meyer-ter-

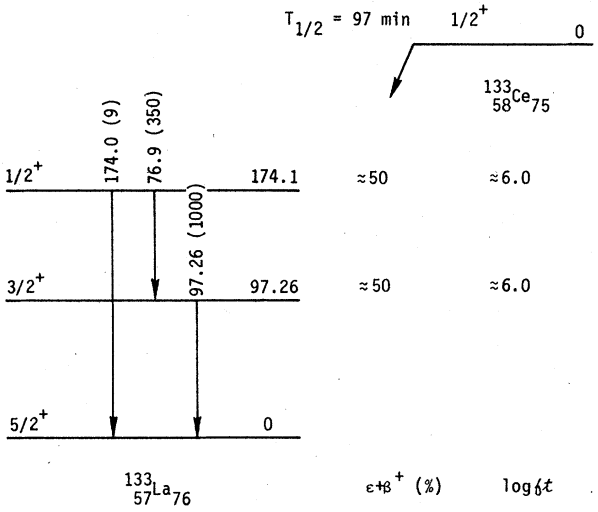

FIG. 4. The decay of the 97-min isomer of ^{133}Ce.

Vehn.[14] The first calculation (a) uses "standard" parameters[14] derived from the energy levels of ^{132}Ba and ^{134}Ce where the effective Fermi surface parameter $\tilde{\lambda}_F$ has been fitted to reproduce the energy of the $\frac{9}{2_1}^-$ level. In the second calculation (b), γ was set to 0° and β was fitted to reproduce the energy of the $\frac{15}{2_1}^-$ level. Then, λ_F was fitted to reproduce the energy of the $\frac{9}{2_1}^-$ level. The energy of the $\frac{9}{2_1}^-$ level increases for $\tilde{\lambda}_F < 1.0$ (the position of the $\frac{15}{2_1}^-$ level is insensitive to $\tilde{\lambda}_F$).

We see that the calculation with the standard parameters is significantly better than the calculation with $\gamma = 0°$. The levels are more compressed for $\gamma = 23.5°$ and are much closer in energy to the experimental levels. More importantly, the level ordering is better with the standard parameter calculation than with the $\gamma = 0°$ calculation. The $\frac{11}{2_1}^-$ level is below the $\frac{19}{2_1}^-$ level, not above it; the $\frac{13}{2_1}^-$ level is closer to the $\frac{15}{2_1}^-$ level than to the $\frac{19}{2_1}^-$ level;

TABLE IV. Summary of the experimental evidence for spins and parity assignments to ^{133}La excited levels.

Level	J^π	Reasons for J^π assignment
495	$\frac{7}{2}^+(\frac{5}{2}^+)$	logft; 346γ is $E2, M1$; no γ ray to $\frac{1}{2}^+$ level.
541	$\frac{7}{2}^+(\frac{5}{2}^+)$	1494γ is $E1$; γ ray to $\frac{3}{2}^+$ level; no γ ray to $\frac{1}{2}^+$ level.
563	$\frac{9}{2}^+(\frac{7}{2}^+,\frac{5}{2}^+)$	432γ is $E2$ (+$M1$); logft; no γ ray to $\frac{3}{2}^+$ level.
654	$\frac{11}{2}^+$	523γ is $E2$; no γ rays to $\frac{3}{2}^+$ or $\frac{5}{2}^+$ levels.
784	$\frac{7}{2}^-$	logft; 784γ is $E1$.
867	$\frac{7}{2}^+(\frac{5}{2}^+)$	logft; γ ray to $\frac{3}{2}^+$ level; no γ ray to $\frac{1}{2}^+$ level.
950	$\frac{9}{2}^+(\frac{7}{2}^+,\frac{5}{2}^+)$	819γ is $M1$ (+$E2$); no γ ray to $\frac{3}{2}^+$ level.
980	$\frac{15}{2}^-$	(HI, $Xn\gamma$) reactions.
1045	$\frac{9}{2}^-$	logft; 510γ is $M1$; γ ray to $\frac{7}{2}^+$ level.
1092	$\frac{7}{2}^+,\frac{9}{2}^+$	γ rays to $\frac{5}{2}^+$ and $\frac{11}{2}^+$ levels.
1153	$\frac{13}{2}^-$	617γ is $M1$; γ rays to no other levels.
1218	$\frac{7}{2}^+(\frac{5}{2}^+)$	logft; γ ray to $\frac{3}{2}^+$ level but not $\frac{1}{2}^+$ level.
1310	$\frac{7}{2}^-\frac{11}{2}$	logft; γ ray to $\frac{11}{2}^+$ level.
1365	$\frac{9}{2}^-,\frac{11}{2}^-$	829γ is $M1$ (+$E2$); γ ray to $\frac{7}{2}^+$ level.
1396	$\frac{5}{2}^-(\frac{7}{2}^-,\frac{9}{2}^-)$	611γ is $M1$; β feeding consistent with zero, all other $\frac{7}{2}^-$ or $\frac{9}{2}^-$ levels have demonstrable β feeding.
1468	$\frac{7}{2}^-,\frac{9}{2}^-$	γ rays to $\frac{7}{2}^-$ and $\frac{13}{2}^-$ levels.
1561	$\frac{11}{2}^-$	logft, transition to $\frac{15}{2}^-$.
1690	$\frac{9}{2}^-(\frac{11}{2}^-)$	644γ is $M1$ (+$E2$); γ rays to $\frac{11}{2}^+$ and $\frac{5}{2}^-(\frac{7}{2}^-,\frac{9}{2}^-)$ levels.
1715	$\frac{7}{2}^-,\frac{9}{2}^-$	1584γ is $E1$, logft.
1734?	$(\frac{11}{2}^-)$	γ ray to $\frac{15}{2}^-$.
1735	$\frac{9}{2}^-(\frac{11}{2}^-)$	689γ is $M1$ (+$E2$); γ rays to $\frac{11}{2}^+$ and $\frac{5}{2}^-(\frac{7}{2}^-,\frac{9}{2}^-)$ levels.
1748	$\frac{7}{2},\frac{9}{2}$	log$f^{1u}t$ γ rays to $\frac{7}{2}^-,\frac{9}{2}^-$, and $\frac{7}{2}^+(\frac{5}{2}^+)$ levels.
1753	$\frac{7}{2}-\frac{11}{2}(\frac{5}{2}^+)$	log$f^{1u}t$.
1784	$\frac{7}{2}-\frac{11}{2}$	log$f^{1u}t$, γ ray to $\frac{11}{2}^+$ level.
1806	$\frac{9}{2},\frac{11}{2}$	log$f^{1u}t$, γ rays to $\frac{11}{2}^+$ and $\frac{11}{2}^-$ levels.
1850	$\frac{7}{2}^+,\frac{9}{2}^\pm$	logft; γ rays to $\frac{7}{2}^+,\frac{7}{2}^-$ and $\frac{11}{2}^+$ levels.
1857	$\frac{7}{2}^-$	logft; 1769γ is $E1$.
1912	$\frac{7}{2}^-,\frac{9}{2}^-$	logft; 1377γ is $E2$ (+$M1$); 1782γ is $E1$.
1958	$\frac{9}{2}^-,\frac{11}{2}^\pm$	log$f^{1u}t$; γ ray to $\frac{13}{2}^-$.
1967	$\frac{7}{2}^-,\frac{9}{2}^\pm$	logft; γ ray to $\frac{7}{2}^+$ and $\frac{11}{2}^-$ levels.
1983	$\frac{7}{2}-\frac{11}{2}$	logft.
2018	$\frac{7}{2}^-$	972γ is $M1$; γ ray to $\frac{5}{2}^+$ level.
2029	$\frac{7}{2},\frac{9}{2}^+$	logft; γ ray to $\frac{5}{2}^+$ level.
2035	$\frac{7}{2}-\frac{11}{2}$	logft.
2036	$\frac{7}{2}^-,\frac{9}{2}^-$	1500γ is $E2$ (+$M1$); γ ray to $\frac{7}{2}^+$ level.
2062	$\frac{7}{2}^-,\frac{9}{2}^-$	1526γ and 1277γ are $E2$ (+$M1$).
2122	$\frac{9}{2}^-\frac{11}{2}$	log$f^{1u}t$; γ ray to $\frac{13}{2}^-$ level.
2132	$\frac{7}{2},\frac{9}{2}^+$	logft; γ ray to $\frac{5}{2}^+$ level.
2137	$\frac{9}{2}^-(\frac{11}{2}^\pm)$	logft; γ rays to $\frac{13}{2}^-$ and $\frac{5}{2}^-(\frac{7}{2}^-,\frac{9}{2}^-)$ levels.
2155	$\frac{9}{2}^-(\frac{9}{2}^+,\frac{11}{2}^\pm)$	logft; γ rays to $\frac{13}{2}^-$ and $\frac{5}{2}^-(\frac{7}{2}^-,\frac{9}{2}^-)$ levels.
2175	$\frac{9}{2}^-,\frac{11}{2}^\pm$	logft; γ ray to $\frac{13}{2}^-$ level.
2200	$\frac{9}{2}^+$	1664γ is $E1$; γ ray to $\frac{5}{2}^+$ level.
2249	$\frac{7}{2}^+,\frac{9}{2}^\pm$	logft; γ ray to $\frac{7}{2}^+,\frac{7}{2}^-$, and $\frac{11}{2}^+$ levels.
2360	$\frac{7}{2}-\frac{11}{2}$	logft.
2367	$\frac{7}{2}^\pm,\frac{9}{2}^\pm$	logft; γ ray to $\frac{5}{2}^+$ level.
2501	$\frac{9}{2}^-,\frac{11}{2}^+$	logft; γ ray to $\frac{13}{2}^-$ and $\frac{7}{2}^+(\frac{5}{2}^+)$ levels.
2851	$\frac{9}{2}^-,\frac{11}{2}^+$	logft; γ ray to $\frac{13}{2}^-$ and $\frac{7}{2}^+$ levels.

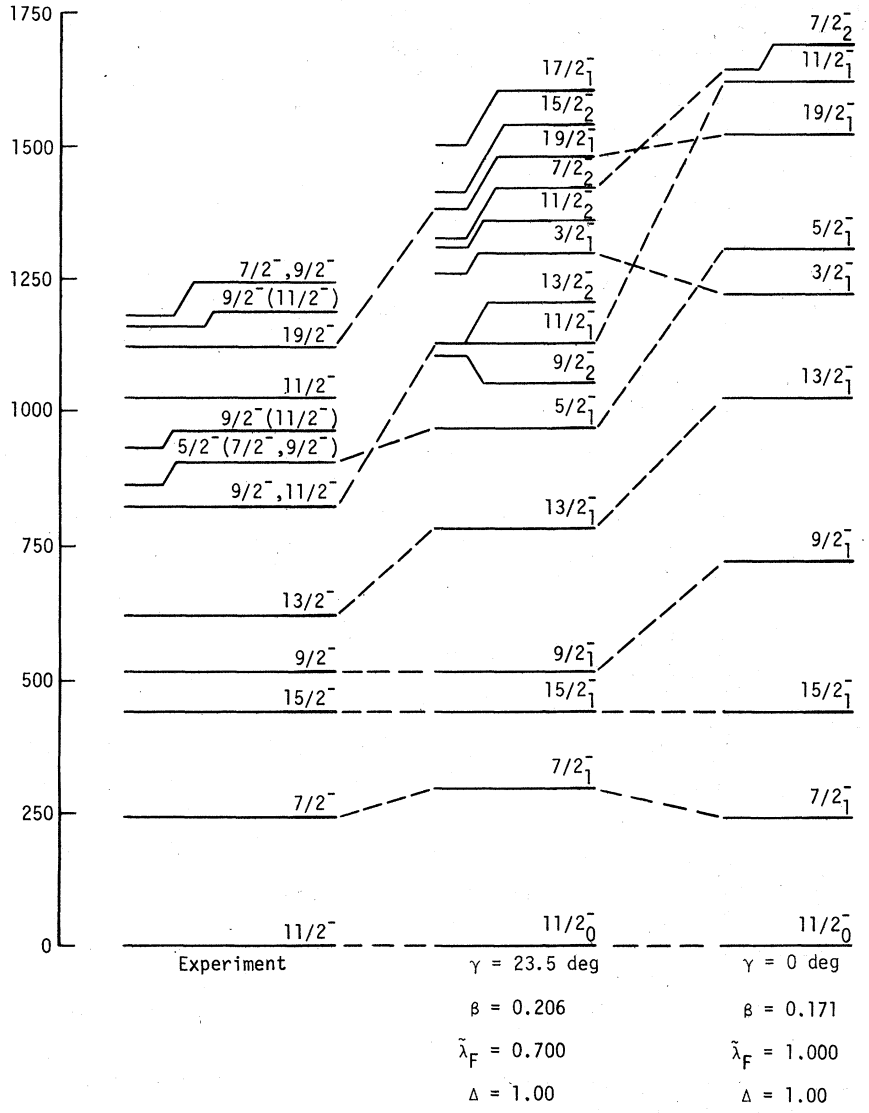

FIG. 5. The experimental negative parity levels up to approximately 1750 keV (a) are compared with calculations using the particle-plus-triaxial-rotor model (b) and the particle-plus-symmetric-rotor model (c).

and the level density has increased dramatically near the $\frac{19}{2_1}^-$ level. This last phenomenon results from two effects. First, in the $\gamma = 0°$ calculation, levels with $j = \frac{7}{2}, \frac{9}{2}$ (resulting from the coupling of the $h_{11/2}$ orbital to the 4_1^+ core state) rise very rapidly in energy with increasing deformation. Second, for $\gamma = 23.5°$ the 2_2^+ core state is near the 4_1^+ core state, resulting in additional levels with $j = \frac{7}{2}, \ldots, \frac{15}{2}$ in the vicinity of the $\frac{19}{2_1}^-$ level.

Although the levels calculated with $\gamma = 23.5°$ compare favorably with our experimental results, the levels of higher energy are still somewhat higher than the experimental values. Toki and Faessler[39] have calculated the levels of ^{133}La using a particle-plus-triaxial-core model but with a variable-moment-of-inertial treatment of the core. This method results in a closer quantitative agreement between theory and experiment for the yrast levels and in a corresponding compression for the lower spin levels. A compression of levels also can occur when higher orders of R^2 are included in the rotational Hamiltonian.[10]

A comparison between triaxial-rotor and symmetric-rotor calculations of transition rate ratios are given in Table V for the $\frac{9}{2_1}$, $\frac{13}{2_1}$, $\frac{11}{2_1}$, and $\frac{5}{2_1}$ levels. The values from the triaxial-rotor calculation are within a factor of 2 to 4.4 of the experimental values for the given ratios. The symme-

TABLE V. Values of experimental transition rate ratios compared with those calculated using a particle-plus-triaxial-rotor and a particle-plus symmetric rotor.

Level	J^π	Transition rate Ratio	Expt.	Triaxial rotor Theory	Triaxial rotor Expt./Theory	Symmetric rotor Theory	Symmetric rotor Expt./Theory
1045	$\frac{9}{2}^-_1$	$\frac{\frac{9}{2}_1 \to \frac{7}{2}_1}{\frac{9}{2}_1 \to \frac{11}{2}_0}$	0.089	0.22	0.40	0.24	0.37
1153	$\frac{13}{2}^-_1$	$\frac{\frac{13}{2}_1 \to \frac{15}{2}_1}{\frac{13}{2}_1 \to \frac{11}{2}_0}$	<0.056	0.61	...	0.61	...
1365	$\frac{11}{2}^-_1$	$\frac{\frac{11}{2}^-_1 \to \frac{9}{2}_1}{\frac{11}{2}_1 \to \frac{11}{2}_0}$	0.32	1.41	0.23	1.85	0.17
		$\frac{\frac{11}{2}_1 \to \frac{13}{2}_1}{\frac{11}{2}_1 \to \frac{11}{2}_0}$	0.30	0.60	0.50	0.75	0.40
		$\frac{\frac{11}{2}_1 \to \frac{9}{2}_1}{\frac{11}{2}_1 \to \frac{11}{2}_0}$	1.1	2.4	0.46	2.5	0.44
		$\frac{\frac{11}{2}_1 \to \frac{7}{2}_1}{\frac{11}{2}_1 \to \frac{11}{2}_0}$	<0.04	0.039	...	0.038	...
1396	$\frac{5}{2}^-_2$	$\frac{\frac{5}{2}_2 \to \frac{9}{2}_1}{\frac{5}{2}_2 \to \frac{7}{2}_1}$	<0.035	0.029	...	0.0114	...

tric-rotor calculation yields very similar results. Taken as a whole, however, the ratios calculated with the triaxial rotor give slightly better agreement with the experiment than do those calculated with the symmetric rotor.

A number of negative parity levels with $j=\frac{7}{2}, \frac{9}{2}$, or $\frac{11}{2}$ are found experimentally between 1400 and 1750 keV. Efforts to correlate these levels with those calculated near the $\frac{19}{2}^-_1$ level have not been completely successful. In general, however, correspondence can be found between experimental and theoretical levels on the basis of relative energy. For example, the 1468.90-, 1561.3-, and 1715.41-keV levels could correspond to the $\frac{9}{2}_2$, $\frac{11}{2}_2$, and $\frac{7}{2}_2$ levels, respectively, which are predicted by the particle-plus-triaxial-core calculation. When the transition rates are considered, however, it is typically found in experiment that one transition from such levels is substantially weaker or stronger than is predicted by theory.

B. Positive parity levels

The main features of the $N=76$ systematics, shown in Fig. 6, are similar to those of the $N=78$ nuclei. First, the level structures are compressed as pairs of protons are added to ^{127}Sb. Next, a second low-lying $\frac{5}{2}^+$ level usually associated with multiparticle effects becomes evident as pairs of protons are added. Third, $\frac{1}{2}^+_1$ and $\frac{3}{2}^+_1$ levels are compressed well below the first phonon energy of the core nucleus. Finally, the $\frac{7}{2}^+_0$ to $\frac{5}{2}^+_0$ transition exhibits the typical hindered $M1$ characteristic of l-forbidden transitions between $1g_{7/2}$ and $2d_{5/2}$ single-particle levels.[47] However, significant differences between the $N=76$ and $N=78$ nuclei also are apparent. The crossover where the $2d_{5/2}$ level replaces the $1g_{7/2}$ level as the ground state occurs between $Z=53$ and 55 in $N=76$ nuclei, but between $Z=55$ and 57 in $N=78$ nuclei. The low-lying $\frac{1}{2}^+_1$ and $\frac{3}{2}^+_1$ levels are compressed much more below

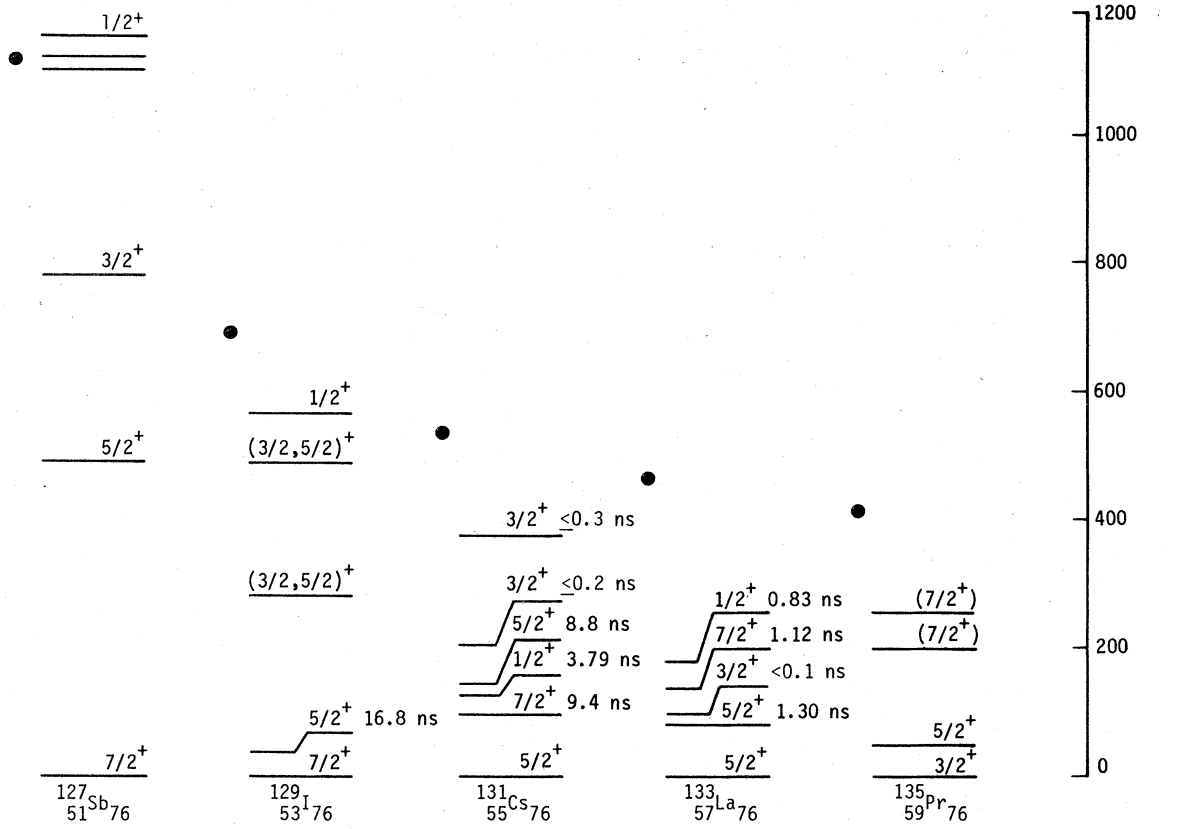

FIG. 6. The systematics of the low-lying positive parity levels in $N=76$ nuclei. (Data taken in part from Refs. 40–42.)

the core phonon energy in the $N=76$ nuclei than in the $N=78$ nuclei. The low-lying $\frac{3}{2}_1^+$ state has become the ground for ^{135}Pr ($N=76$), whereas in ^{137}Pr, the $\frac{3}{2}_1^+$ level is rising in energy when compared to the $\frac{3}{2}_1^+$ level in ^{135}La. Finally, the $\frac{1}{2}_1^+$ levels in ^{133}La and ^{135}La appear to behave differently. However, as we will detail later, there is reason to suspect that the half-life of the $\frac{1}{2}^+$ level in ^{133}La is in error (see Table VI).

In Fig. 7, we show the $Z=57$ systematics, including the low-lying positive parity levels and the $\frac{11}{2}^-$ level which is largely $h_{11/2}$ in nature. These systematics clearly illustrate the compression of the level structure, with $\frac{1}{2}_1^+$ and $\frac{3}{2}_1^+$ levels dropping well below the core phonon energy. The lowest $\frac{9}{2}^+$ and $\frac{11}{2}^+$ levels are found near the core phonon energy. The hindrances of the $E1$, $M1$, and $M2$ transitions and the enhancements of the $E2$ and $E3$ transitions out of the $\frac{11}{2}_0^-$ level to lower positive parity levels are given in Table VII. The most noticeable trends are the increased hindrance of the $\frac{11}{2}_0^-$ to $\frac{7}{2}_0^+$ $M2$ and the decreased enhancement of the $\frac{11}{2}_0^-$ to $\frac{5}{2}_0^+$ $E3$ transition as neutron pairs are removed from ^{139}La. It has been suggested that the $E3$ enhancement of the $\frac{11}{2}_0^-$ to $\frac{5}{2}_0^+$ transition in ^{137}La is due to the participation of the octupole vibration.[48] However, because the 3^- octupole state in the even-even Ba nuclei is slowly decreasing in energy with decreasing A, and because the $\frac{11}{2}_0^-$ level retains its $h_{11/2}$ single-particle character, the decreases in the $E3$ transition rate can be attributed to the changing nature of the $\frac{5}{2}_0^+$ level. Thus the $2d_{5/2}$ single-particle state may contribute less to the $\frac{5}{2}_0^+$ level in ^{129}La than in the heavier La nuclei.

Nuclear models, including weak-coupling, three-particle models with phonon coupling, and the "dressed" three-quasiparticle model, have been invoked to describe nuclei with $A=133$. These models have been discussed extensively in relation to ^{135}La and thus will be reviewed only briefly here. In general, each of these models explains the level structure of ^{133}La less successfully than that of the La nuclei nearer closed shells.

The weak-coupling model[52] has successfully explained the levels of odd-mass nuclei near closed shells (e.g., ^{137}La). The weak-coupling model can account for the $\frac{9}{2}^+$ and $\frac{11}{2}^+$ levels as well as for numerous other positive parity levels near the first phonon energy which are observed in ^{137}La. However, the clustering of the $\frac{5}{2}_1^+$, $\frac{3}{2}_1^+$, and $\frac{1}{2}_1^+$ levels

TABLE VI. $M1$ hindrances and $E2$ enhancements for transitions in $N = 76$ nuclei. On the basis of our decay scheme, the level half-life attributed to a 742-keV level by Ref. 21 is actually the half-life of the $\frac{5}{2}^+_1$ level at 87 keV.

Transition		^{129}I[a]	^{131}Cs[b]	^{133}La[c]
$\frac{7}{2}^+_0 \rightleftarrows \frac{5}{2}^+_0$	$H(M)$[d]	100	600	210-250
	$E(E2)$[e]	25	0.63	26-31[f]
$\frac{5}{2}^+_1 \rightarrow \frac{5}{2}^+_0$	$H(M1)$	...	6400	110
	$E(E2)$	...	1.5	...
$\frac{1}{2}^+_1 \rightarrow \frac{5}{2}^+_0$	$E(E2)$	...	67	0.81[g]
$\frac{1}{2}^+_1 \rightleftarrows \frac{3}{2}^+_1$	$H(M1)$	...	$\leqslant 16$	58
	$E(M1)$	...	$\geqslant 170$	...
$\frac{3}{2}^+_1 \rightarrow \frac{5}{2}^+_0$	$H(M1)$	...	$\leqslant 110$	<9.4
	$E(E2)$	...	$\geqslant 1.2$	...

[a] Data from Ref. 43.
[b] Data from Refs. 44 and 45.
[c] Data from present experiment and Ref. 29.
[d] $T_{1/2}$(expt)/$T_{1/2}$(Weisskopf estimate).
[e] $T_{1/2}$(Weisskopf estimate)/$T_{1/2}$(expt.).
[f] Assuming $\delta^2 = 0.176$; $\delta^2 \leqslant 0.03$ from L_1/L_2 conversion-electron ratio of Ref. 17.
[g] See text.

in ^{133}La near the ground state cannot be explained by weak coupling.

The application of the cluster-plus-vibrational-field model has led to success in calculations of I and Ce nuclei,[53-55] particularly near $N = 82$. For Ce nuclei, however, the agreement between theory and experiment deteriorates as N decreases. Calculations of the La nuclei using cluster-plus-vibrational-field models have not been undertaken.

A microscopic theory of collective excitations, i.e., the dressed quasiparticle formalism, has been developed by Kuriyama *et al.*[56-59] to describe the low-lying $\frac{5}{2}^+$ and $\frac{3}{2}^+$ states in spherical nuclei. This formalism treats consistently both types of lowest order perturbation effects that are necessary to calculate the properties of excited states composed of one quasiparticle and one phonon. These effects (Fig. 8) are the conventional diagram that usually is treated as phonon-quasiparticle coupling [Fig. 8(a)] and the diagram that explicitly accounts for the Pauli principle [Fig. 8(b)]. (See Refs. 56 and 60, Chap. 3, for a detailed discussion.)

Using the dressed three-quasiparticle formalism with a pairing-plus-quadrupole force, Kuriyama *et al.* have calculated energies and reduced transition probabilities for the low-lying $\frac{5}{2}^+_1$ and $\frac{3}{2}^+_1$ lev-

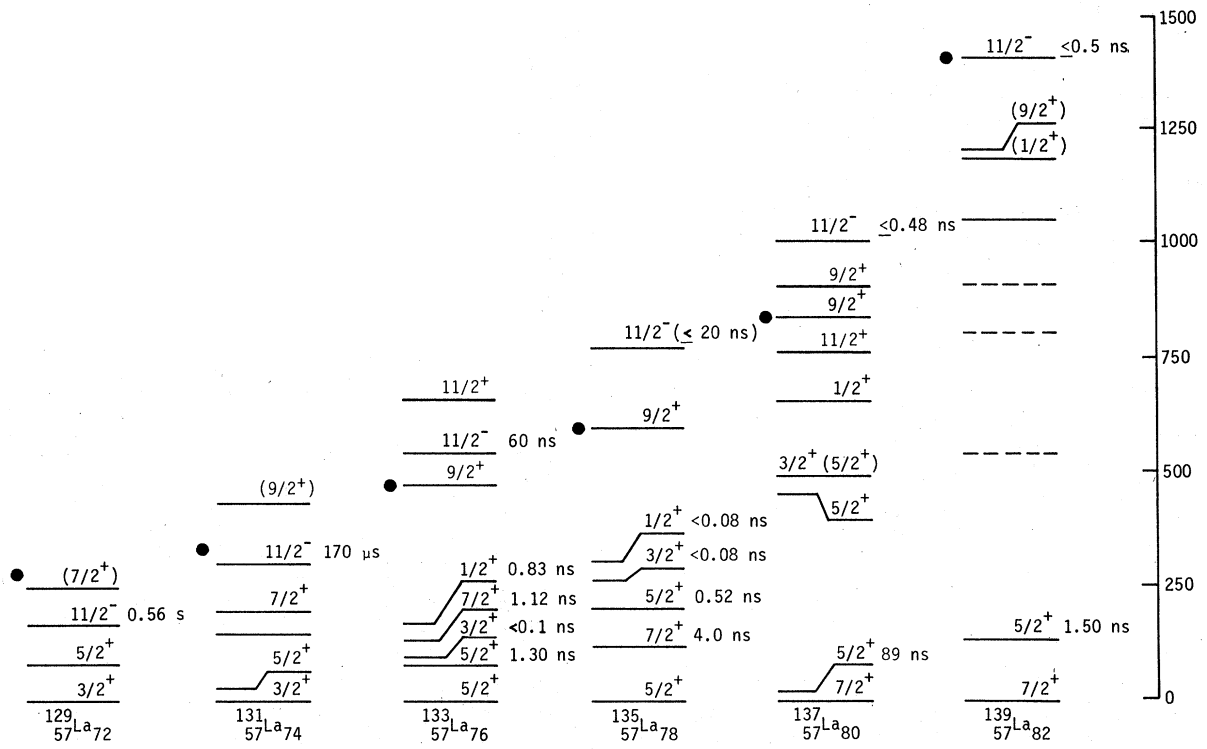

FIG. 7. The $Z = 57$ systematics of the low-lying positive parity levels and the lowest $\frac{11}{2}^-$ level.

TABLE VII. Transition hindrances or enhancements for $Z = 57$ nuclei.

Transition		^{129}La[a]	^{131}La[a]	^{133}La[b]	^{135}La[c]	^{137}La[d]	^{139}La[e]
$\frac{7}{2}^+_0 \rightleftarrows \frac{5}{2}^+_0$	$H(M1)$[f]	...	...	210-250	540	≈670	390
	$E(E2)$[g]	...	...	...	...	...	⩽0.20
$\frac{11}{2}^-_0 \rightarrow \frac{7}{2}^+_0$	$H(M2)$[f]	...	19	13-19	...	⩽10.6	⩽2.5
	$E(E3)$[g]	...	...	⩽139	...	⩾4.6	...
$\frac{11}{2}^-_0 \rightarrow \frac{5}{2}^+_0$	$E(E3)$[g]	0.72	...	4.3	...	⩾9.1	...
$\frac{11}{2}^-_0 \rightarrow \frac{9}{2}^+_1$	$H(E1)$[f]	...	...	9.8×10^4	$\leqslant 6.6 \times 10^5$	$\leqslant 1.03 \times 10^4$	...

[a] Data from Ref. 8.
[b] Data from present experiment and Ref. 29.
[c] Data from Refs. 1, 8, and 46.
[d] Data from Refs. 2, 48, and 49.
[e] Data from Refs. 50 and 51.
[f] $T_{1/2}$(expt)/$T_{1/2}$(Weisskopf estimate).
[g] $T_{1/2}$(Weisskopf estimate)/$T_{1/2}$(expt.)

els in $^{131-137}$La.[59,60] The level energies calculated by Kuriyama *et al.* using two estimates of the quadrupole-force strength are reproduced in Fig. 9 (Ref. 60, Chap. 4). Calculated reduced transition probabilities and their ratios for which experimental data are available are summarized in Table VIII. The theoretical results are given for cases with and without coupling between the dressed three-quasiparticle and one-quasiparticle modes.

A comparison of the level energies calculated by Kuriyama *et al.* (Fig. 9) with the experimental La levels (Fig. 7) reveals that the calculation reproduces the general trend of the $\frac{5}{2}^+_1$ and $\frac{3}{2}^+_1$ levels. In particular, the agreement for ^{137}La is quite good when a small shift of the single-particle energies is taken into account. However, the detailed agreement between theory and experiment deteriorates substantially for ^{135}La and ^{133}La. It is evident, however, that the calculated energies are very sensitive to the quadrupole-force strength.

It is of interest nevertheless to compare the reduced transition rates and their ratios with the experimental data available and to examine trends as neutron pairs are removed from ^{137}La (Table VIII). Reduced transition probabilities are calculated by Kuriyama *et al.*, both with and without coupling effects (Ref. 60, Chap. 4). First, we can see that the experimental ratio of the $B(E2)$ values for transitions out of the $\frac{5}{2}^+_1$ level to the $\frac{5}{2}^+_0$ and $\frac{7}{2}^+_0$ levels is substantially larger than the calculated ratio for both ^{135}La and ^{137}La. A similar effect is seen for transitions out of the $\frac{3}{2}^+_1$ level, although

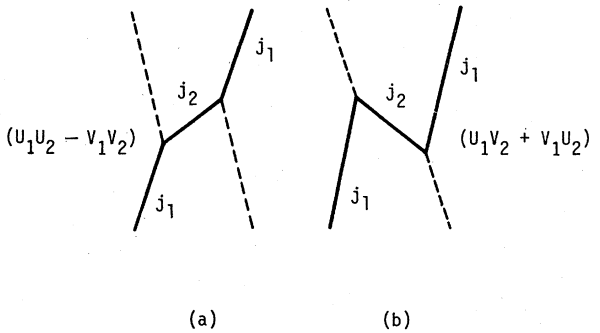

FIG. 8. The conventional lowest order diagram that is usually treated as phonon-quasiparticle coupling (a) and the lowest order diagram that explicitly takes into account the Pauli principle (b).

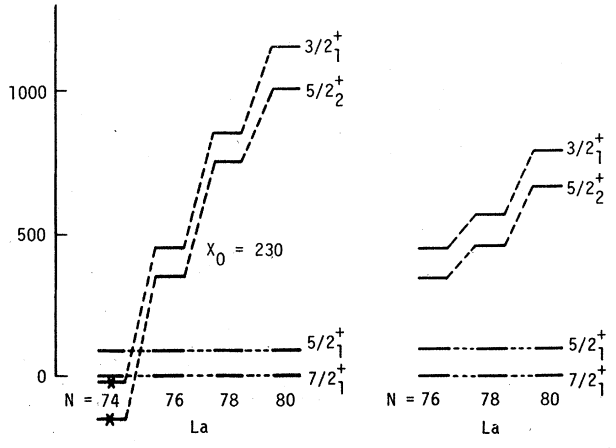

FIG. 9. The levels of odd-mass La nuclei as calculated by Kuriyama *et al.* In (a) a constant quadrupole-force-strength parameter of $X_0 = 230$ is used; in (b) the value of X_0 is chosen to reproduce the average energies of the 2^+ phonons in the adjacent even-even nuclei.

in this case, the effect of coupling improves the agreement between theory and experiment. We note that the $B(E2)$ value for the transition from the $j-1$ state to the j state is not affected greatly by the inclusion of coupling because the anomolous-coupling-like component of the $j-1$ state remains dominant. Other transitions, where the matrix elements are small, are sensitive to small admixtures (Ref. 60, Chap. 4). Compared with the transitions to the $\frac{7}{2}_0^+$ level, transitions from the $\frac{3}{2}_1^+$ and $\frac{5}{2}_0^+$ levels are more collective than the calculations by Kuriyama *et al.* would suggest for both ^{137}La and ^{135}La.

The $B(M1)$ values for both ^{135}La and ^{133}La have been calculated by Kuriyama *et al.* and are in good agreement with our experimental values. This agreement reflects the success with which the coupling among low-lying states has been carried out. Unfortunately, the lack of accurate mixing ratios for transitions between low-lying levels in ^{133}La precludes any comparison with calculated $B(E2)$ values for that nucleus.

In addition, further comment is needed on the rapid descent of the $\frac{1}{2}_1^+$ level in La nuclei with decreasing mass. As currently formulated, the dressed quasiparticle theory does not calculate the $\frac{1}{2}_1^+$ level at this low energy. Although the coupling among modes with different transferred seniority quantum numbers can lower the $\frac{1}{2}_1^+$ energy somewhat, the main influence for this level would come from the inclusion of dressed five-quasiparticle configurations (Ref. 60, Chap. 3). Below, we discuss the influence of the $s_{1/2}$ state through its interaction with the $\frac{1}{2}^+|d_{5/2}2_1\rangle$ configuration (via the nonspin-flip matrix element).

Thus overall, the dressed three-quasiparticle theory explains rather well the properties of the La nuclei near the $N=82$ closed shell. In particular, the behavior of the $\frac{5}{2}_1^+$ level is reproduced with some success. On the basis of the level energies, however, this theory may not be applicable in detail to ^{133}La and lighter La nuclei. Kuriyama *et al.* point out that when the $j-1$ state (the $\frac{5}{2}_1^+$ level in this case) falls below the j state (the $\frac{7}{2}_0^+$ level), a growth of instability toward quadrupole deformation is indicated (Ref. 60, Chap. 3). In ^{133}La, the $\frac{5}{2}_1^+$ level does fall below the $\frac{7}{2}_0^+$ level. As a result, the applicability of the dressed three-quasiparticle theory to ^{133}La should be regarded as suspect.

We have shown that the particle-plus-triaxial-rotor model successfully accounts for the properties of the decoupled system arising out of the $h_{11/2}$ orbital.[3,4] This success has led us to consider

TABLE VIII. Reduced transition rates and their ratios for transitions that have experimental data available. The theoretical values are from Kuriyama *et al.* (Ref. 60) for cases with coupling effects (value in parentheses) and without coupling effects.

	Nuclide	Theory	Experiment[a]	Experiment/Theory
$\frac{B(E2;\frac{5}{2}_1^+\to\frac{5}{2}_0^+)}{B(E2;\frac{5}{2}_1^+\to\frac{7}{2}_0^+)}$	^{137}La	0.029 (0.029)	0.25[b]	8.6 (8.6)
	^{135}La	0.041 (0.021)	0.13	3.2 (6.2)
$B(E2;\frac{5}{2}_1^+\to\frac{5}{2}_0^+)$	^{135}La	0.4 (0.2)	1.8	4.5 (9.0)
$B(E2;\frac{5}{2}_1^+\to\frac{7}{2}_0^+)$	^{135}La	9.7 (9.6)	13.5	1.4 (1.4)
$\frac{B(E2;\frac{3}{2}_1^+\to\frac{7}{2}_0^+)}{B(E2;\frac{3}{2}_1^+\to\frac{5}{2}_0^+)}$	^{135}La	0.075 (0.038)	0.022	0.29 (0.58)
$B(E2;\frac{3}{2}_1^+\to\frac{5}{2}_0^+)$	^{135}La	9.3 (8.4)	>5.0	...
$B(E2;\frac{3}{2}_1^+\to\frac{7}{2}_0^+)$	^{135}La	0.7 (0.32)	>0.11	...
$B(M1;\frac{5}{2}_1^+\to\frac{7}{2}_0^+)$	^{135}La	... (0.0021)	0.0027	(1.3)
$B(M1;\frac{5}{2}_1^+\to\frac{5}{2}_0^+)$	^{135}La	... (0.0026)	0.0064	(2.5)
	^{133}La	... (0.010)	0.017	(1.7)

[a] Data from this work and previously cited references.

[b] The multipolarity of the $\frac{5}{2}_1^+$ to $\frac{7}{2}_0^+$ transition is approximately 33% $M1$ + 67% $E2$ from the conversion electron data (see Ref. 2).

whether the positive parity levels can be accounted for by a decoupled system built on the $d_{5/2}$ and $g_{7/2}$ orbitals. To test this on the simplest possible model, we have assumed as a starting hypothesis that the $d_{5/2}$ particle and the $g_{7/2}$ hole do not interact to a significant degree. Thus, the $d_{5/2}$ and $g_{7/2}$ systems are calculated separately using the particle-plus-triaxial-rotor model. Shown in Fig. 10 are the energy levels resulting from these calculations. In the first column, we give the experimental positive parity levels below 1 MeV and several levels for which J^π values are not known, but which are expected to have positive parity. The third and fourth columns list, respectively, the levels calculated for a $g_{7/2}$ proton hole (because the $g_{7/2}$ orbital should be largely filled) and for a $d_{5/2}$ proton particle. The deformation parameters were $\beta = 0.206$ and $\gamma = 23.5°$, the same as for the negative parity levels. In each case, the Fermi energy was fit to the $j-1$ level. After arbitrarily adjusting the $\frac{7}{2}_0^+$ level to match our experimental value, the cumulative calculated level structure was obtained (see column 2, Fig. 10). Thus we see that the energies of the $\frac{9}{2}_1^+$ and $\frac{11}{2}_1^+$ levels corresponding

TABLE IX. Comparison of the transition rate ratios and reduced transition rates from experiment with calculations using the particle-plus-triaxial-rotor model. Mixing between the $d_{5/2}$ and $g_{7/2}$ families of levels is not included.

Level	J^π	Quantity	Experiment	Theory[b]	Experiment/Theory
97	$\frac{3}{2}^+$	$B(M1, \frac{3}{2}_1 \rightarrow \frac{5}{2}_0)$	>0.19[c]	0.52	...
174	$\frac{1}{2}^+$	$B(E2, \frac{1}{2}_1 \rightarrow \frac{5}{2}_0)$	0.0033	0.2559	0.013
		$B(M1, \frac{1}{2}_1 \rightarrow \frac{3}{2}_1)$	0.031[c]	3.6765	0.0084
		$\frac{T(\frac{1}{2}_1 \rightarrow \frac{3}{2}_1)}{T(\frac{1}{2}_1 \rightarrow \frac{5}{2}_0)}$	100	58	1.72
495	$\frac{7}{2}^+$	$\frac{T(\frac{7}{2}_1 \rightarrow \frac{3}{2}_1)}{T(\frac{7}{2}_1 \rightarrow \frac{5}{2}_0)}$	1.0	0.084	12
	$(\frac{5}{2}^+)$	$\frac{T(\frac{5}{2}_1 \rightarrow \frac{3}{2}_1)}{T(\frac{7}{2}_1 \rightarrow \frac{5}{2}_0)}$	1.0	1.17	0.85
541	$\frac{7}{2}^+$	$\frac{T(\frac{7}{2}_1 \rightarrow \frac{3}{2}_1)}{T(\frac{7}{2}_1 \rightarrow \frac{5}{2}_0)}$	2.1	0.106	19.8
	$(\frac{5}{2}^+)$	$\frac{T(\frac{5}{2}_1 \rightarrow \frac{3}{2}_1)}{T(\frac{7}{2}_1 \rightarrow \frac{5}{2}_0)}$	2.1	1.29	1.63
563	$\frac{9}{2}^+$	$\frac{T(\frac{9}{2}_1 \rightarrow \frac{5}{2}_1)}{T(\frac{9}{2}_1 \rightarrow \frac{7}{2}_0)}$	0.89	0.51	1.74
950	$\frac{9}{2}^+$	$\frac{T(\frac{9}{2}_2 \rightarrow \frac{5}{2}_1)}{T(\frac{9}{2}_1 \rightarrow \frac{7}{2}_0)}$	0.77	1.94	0.40
	$(\frac{7}{2}^+)$	$\frac{T(\frac{7}{2}_1 \rightarrow \frac{5}{2}_1)}{T(\frac{7}{2}_1 \rightarrow \frac{7}{2}_0)}$	0.77	10	0.077
	$(\frac{5}{2}^+)$	$\frac{T(\frac{5}{2}_2 \rightarrow \frac{5}{2}_1)}{T(\frac{5}{2}_2 \rightarrow \frac{7}{2}_0)}$	0.77	0.65	1.18

[a] $B(M1)$ values are in μ_N; $B(E2)$ values are in $(e\ \mathrm{b})^2$: see Ref. 2.
[b] Triaxial rotor calculation.
[c] Assuming pure $M1$ transition.

to the first members of the yrast-decoupled band built on the $d_{5/2}$ and $g_{7/2}$ states are accurately predicted. A $\frac{1}{2}_1^+$ level is predicted somewhat lower than the lowest $\frac{9}{2}_1^+$ level while experimentally, the $\frac{1}{2}_1^+$ level is seen substantially lower in energy. Several additional $\frac{5}{2}^+$, $\frac{7}{2}^+$, and $\frac{9}{2}^+$ levels are observed and can be correlated with calculated levels. Also, the $\frac{13}{2}^+$ and $\frac{15}{2}^+$ levels observed by Chiba *et al.*[12] are calculated at 1376 and 1498 keV, respectively. The fact that these levels are found 100 to 200 keV below the calculated energies is consistent with the results for the $\frac{19}{2}^-$ level.

Transition rate ratios and reduced transition rates are summarized for the decay of seven positive parity levels in Table IX. The following correspondences can be made: The 950-keV level could be either the $\frac{9}{2}_2^+$ or $\frac{5}{2}_2^+$ member of the $1g_{7/2}$ family; the 563-keV level is probably the $\frac{9}{2}_1^+$ member of the $1g_{7/2}$ family; and the $\frac{5}{2}_1^+$ member of the $2d_{5/2}$ family could be at either 495 or 541 keV. Based on its energy, the $\frac{7}{2}_1^+$ member of the $2d_{5/2}$ family could be at either 495 or 541 keV; however, there is a 10- to 20-fold difference between theoretical and experimental transition rate ratios if

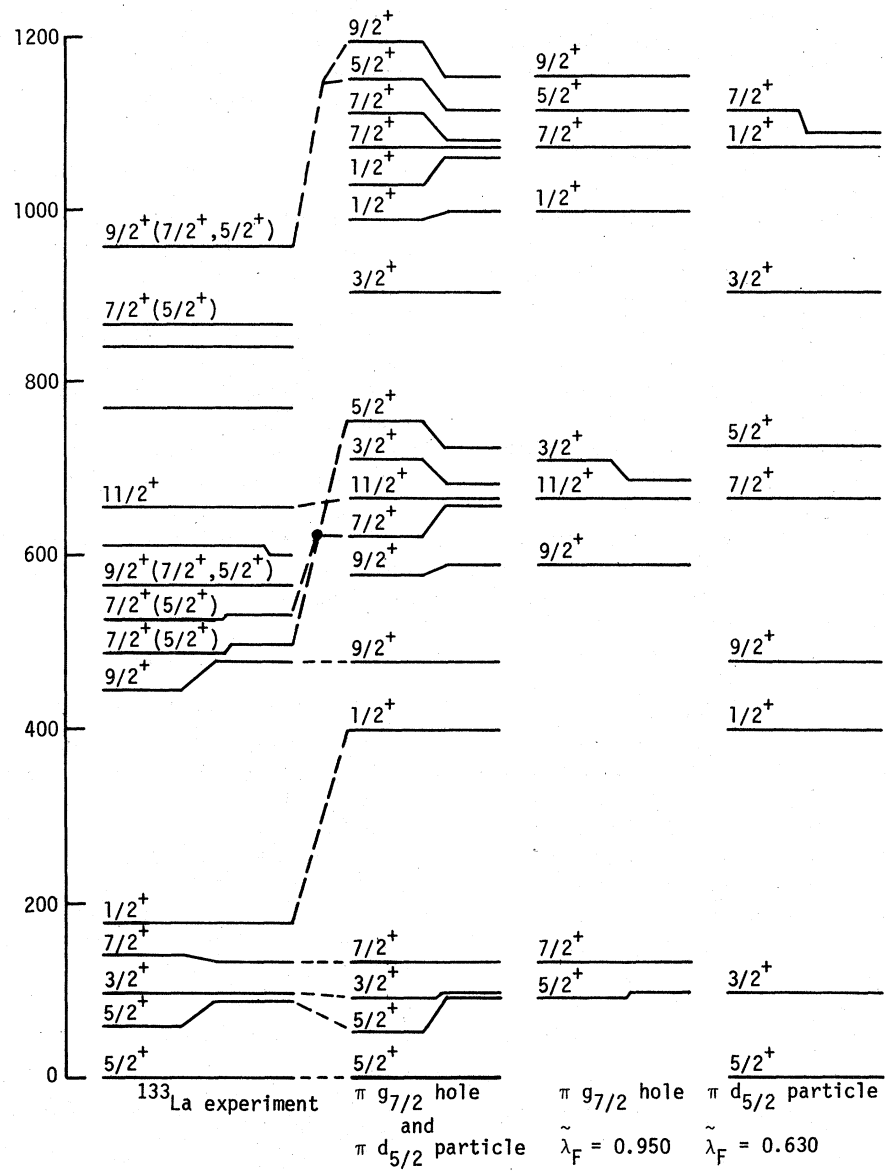

FIG. 10. The low-lying positive parity levels found in this work (a), the cumulative level structure calculated by the particle-plus-triaxial-rotor model when the $\frac{7}{2}^+$ level is arbitrarily adjusted to agree with experimental results (b), as well as the calculation of the $1g_{7/2}$ family (c) and the $2d_{5/2}$ family (d) with the particle-plus-triaxial-rotor model.

either of these levels is $\frac{7}{2}^+$.

The largest apparent discrepancy between experiment and theory appears in the $B(E2)$ and $B(M1)$ values for transitions originating from the $\frac{1}{2}^+$ level to the $\frac{3}{2}^+_1$ and $\frac{5}{2}^+_0$ levels of the $d_{5/2}$ family. The $B(E2)$ value for the 174-keV transition out of the $\frac{1}{2}^+$ level is 0.81 times the single particle $B(E2)$ value (see Table VI) if the half-life of the 174-keV level is 0.83 ns. However, enhancements over the single-particle $B(E2)$ value for corresponding $\frac{1}{2}^+$ to $\frac{5}{2}^+$ transitions in ^{135}La, ^{133}Cs, and ^{131}Cs are ≥ 52, ≥ 12, and 67, respectively. If the $B(E2)$ enhancement for the 174-keV transition was comparable in value to these, the discrepancy between theory and experiment would disappear. A remeasurement of the lifetime of the 174-keV level could clarify this situation.

The discrepancy between the predicted and the experimentally observed energy of the $\frac{1}{2}^+$ level in the $d_{5/2}$ system deserves further mention. The level occurs at a lower energy than is predicted theoretically. This can be understood in terms of the mixing of the $s_{1/2}$ single-particle state (which may be several MeV higher than the $d_{5/2}$ state) with the $\frac{1}{2}^+$ state, resulting from coupling the $d_{5/2}$ single particle to the 2^+_1 core state (e.g., $\frac{1}{2}^+|d_{5/2}2^+_1\rangle$). Configurations such as $\frac{1}{2}^+|d_{5/2}2^+_1\rangle$ are known to interact strongly with their nonspin-flip partners, $\frac{1}{2}^+|s_{1/2}0^+_1\rangle$ in this case, through large nonspin-flip matrix elements.[61,62]

An example of this interaction is known in $^{115}_{49}$In, where the odd proton can be excited above the $Z = 50$ shell closure to the $d_{5/2}$ state. The lowest-lying level resulting from coupling this $d_{5/2}$ proton to the core 2^+_1 state is the $\frac{1}{2}^+$ level. This level has the $\frac{1}{2}^+|s_{1/2}0^+_1\rangle$ configuration as a major component. Such an effect can also be seen in $g_{9/2}$ systems where the odd particle occupies the $g_{9/2}$ single-particle orbital and the $d_{5/2}$ single-particle orbital above it is empty. Then a $\frac{5}{2}^+$ level is at low energy or even becomes the ground state, as in $^{75}_{34}$Se.

In the cluster-plus-vibrational-field model, the interaction of paired nonspin-flip configurations such as those described above increases with increasing particle-core coupling strength. The interaction lowers the $J-2$ level until it becomes lower in energy than the parent J state. A prerequisite for the effect is that the proper single-particle orbital must be available above the parent orbital for occupation by the odd particle or odd hole.

This requirement is most easily seen in hole systems. In Ag nuclei[63-67] where a hole occupies the $g_{9/2}$ orbital, no low-lying $\frac{5}{2}^+$ level is observed, because there is no $d_{5/2}$ hole state at an energy above that of the parent state. Similarly in ^{133}La, the $g_{7/2}$ hole state has no spin-flip partner and the $J-2$ level arising from the $\frac{3}{2}^+|g_{7/2}2^+_1\rangle$ configuration occurs at the unperturbed position (Fig. 10).

Hopefully, calculational approaches being developed by Toki and Faessler[68,69] which treat this interaction for the triaxial nucleus will be able to account for the $J-2$ states in the particle systems such as the decoupled $d_{5/2}$ system of ^{133}La.

V. SUMMARY

We have extended substantially the experimental knowledge of ^{133}La level structure. The particle-plus-triaxial-rotor model enables successful calculations of the properties of the low-lying negative parity states. The dressed three-quasiparticle model and the weak-coupling model do not adequately explain the properties of the low-lying positive parity levels. Calculations applying the particle-plus-triaxial-rotor model to the $2d_{5/2}$ proton particle and the $1g_{7/2}$ proton hole can predict the low-lying positive parity states surprisingly well. If such a calculation included mixing, even better agreement with experiment could reasonably be expected.

ACKNOWLEDGMENTS

The authors thank N. L. Smith for performing the chemistry, and R. J. Dupzyk and C. M. Henderson for performing the mass separations in preparation of the ^{133}Ce sources. The authors also thank F. S. Stephens, G. Alaga, S. G. Nilsson, A. Faessler, and J. Meyer-ter-Vehn for useful discussions. This work was performed under the auspices of the U. S. Department of Energy, by the Lawrence Livermore Laboratory, under contract No. W-7405-Eng-48.

[1] E. A. Henry and R. A. Meyer, Phys. Rev. C 12, 1321 (1975).
[2] E. A. Henry, N. Smith, P. G. Johnson, and R. A. Meyer, Phys. Rev. C 12, 1314 (1975).
[3] E. A. Henry and R. A. Meyer, Z. Phys. 271, 75 (1974).
[4] E. A. Henry and R. A. Meyer, Phys. Rev. C 13, 2063 (1976).
[5] H. Abou-Leila, C. Gerschel, and N. Perrin, Compt. Rend. 265, 1131 (1967).
[6] C. Gerschel, Nucl. Phys. A108, 337 (1968).
[7] C. Gerschel, J. P. Husson, N. Perrin, and L. Valentin, in *Proceedings of the International Conference on Properties of Nuclear States, Montreal, 1969.* (Presses de l'Universite de Montreal, Montreal, Canada, 1969).

[8]J. R. Leigh, K. Nakai, K. H. Maier, F. Puhlohofer, F. S. Stephens, and R. M. Diamond, Nucl. Phys. A213, 1 (1973).
[9]K. Nakai, P. Kleinheinz, J. R. Leigh, K. H. Maier, F. S. Stephens, R. M. Diamond, and G. Lovhoiden, Phys. Lett 44B, 443 (1973).
[10]F. S. Stephens, R. M. Diamond, J. R. Leigh, T. Kammuri, and K. Nakai, Phys. Rev. Lett. 29, 438 (1972).
[11]F. S. Stephens, R. M. Diamond, and S. G. Nilsson, Phys. Lett. 44B, 429 (1973).
[12]J. Chiba, R. S. Hayano, M. Sikimoto, H. Nakayama, and K. Nakai, J. Phys. Soc. Jpn. 43, 1109 (1977).
[13]M. A. Delephanque, C. Gerschel, N. Perrin, and P. Quentin, Phys. Lett. 46B, 317 (1973).
[14]J. Meyer-ter-Vehn, Nucl. Phys. A249, 111, 141 (1975).
[15]H. Toki and A. Faessler, Nucl. Phys. A253, 231 (1975).
[16]P. A. Butler, J. Meyer-ter-Vehn, D. Ward, H. Bertschat, P. Colombani, R. M. Diamond, and F. S. Stephens, Phys. Lett. 56B, 453 (1975).
[17]A. A. Abdumalikov, A. A. Abdurazakov, S.'B. Buribaev, K. Y. Gromov, and N. A. Lebedev, Yad. Fiz. 3, 602 (1966) [Soviet J. Nucl. Phys. 3, 441 (1966)].
[18]A. Abdul-Malek and R. A. Naumann, Nucl. Phys. A108, 401 (1968).
[19]R. Babadzhanov, V. A. Morozov, T. M. Muminov, V. I. Razov, and A. B. Khalikulov, Report No. JINR-P6-5200 1970 (unpublished).
[20]V. Berg, J. Letessier, C. Bourgeois, and R. Foucher, J. Phys. (Paris) 33, 829 (1972).
[21]V. A. Morosov, T. M. Muminov, H. Fuia, and A. B. Khalikulov, Report No. JINR-P6-6635, 1972 (unpublished).
[22]C. Gerschel, N. Perrin, and L. Valentin, J. Phys. (Paris) 34, 753 (1973).
[23]S. Ingelman, C. Ekstrom, M. Olsmats, and B. Wannberg, Phys. Sci. 7, 24 (1973).
[24]B. J. Stover, Phys. Rev. 81, 8 (1951).
[25]R. J. Gehrke and R. G. Helmer, J. Inorg. Nucl. Chem. 38, 1929 (1976).
[26]C. Gerschel, N. Perrin, and L. Valentin, Phys. Lett. 33B, 299 (1970).
[27]M. A. Deleplanque, C. Gerschel, N. Perrin, J. N. Rimbert, and L. Valentin, C. R. Acad. Sci. 273, 565 (1971).
[28]B. Klemme, P. Herzog, G. Schafer, R. Folle, and G. Netz. Phys. Lett. 45B, 38 (1973).
[29]E. A. Henry, Nucl. Data Sheets 11, 495 (1974).
[30]E. A. Henry and R. A. Meyer, Phys. Rev. C 13, 2501 (1976).
[31]R. Gunnick and J. B. Niday, Lawrence Livermore Laboratory, Report No. UCRL-51061, 1971 (unpublished) Vols. I–IV.
[32]D. C. Camp. H. Easterday, L. Nunnelley, and M. Kosty, Bull. Am. Phys. Soc. 21, 632 (1976).
[33]J. B. Niday and L. G. Mann, in *Radioactivity in Nuclear Spectroscopy*, edited by J. H. Hamilton and J. C. Manthuruthil (Gordon and Breach, New York, 1972), Vol. 1, p. 313.
[34]R. S. Hager and E. C. Seltzer, Nucl. Data A4, 1 (1968).
[35]V. F. Trusov, Nucl. Data Tables 10, 477 (1972).
[36]A. H. Wapstra and N. B. Gove, Nucl. Data Tables 9, Nos. 4 and 5 (1971).
[37]H. A. Smith and F. A. Rickey, Phys. Rev. C 14, 1946 (1976).
[38]S. V. Jackson and R. A. Meyer, Bull. Am. Phys. Soc. 21, 633 (1976); (to be published).
[39]H. Toki and A. Faessler, Nucl. Phys. A253, 231 (1975).
[40]R. L. Auble, J. B. Ball, and C. B. Fulmer, Nucl. Phys. A116, 14 (1968).
[41]M. Conjeaud, S. Harar, M. Caballero, and N. Cindro, Nucl. Phys. A215, 383 (1973).
[42]R. L. Auble, Nucl. Data B8, 77 (1972).
[43]D. J. Horen, Nucl. Data B8, 123 (1972).
[44]R. J. Gehrke, R. G. Helmer, C. W. Reich, R. G. Greenwood, and R. A. Anderl, Phys. Rev. C 14, 1896 (1976).
[45]R. L. Auble, H. R. Hiddleston, and C. P. Brown, Nucl. Data Sheets 17, 573 (1976).
[46]E. A. Henry, Nucl. Data Sheets 14, 191 (1975).
[47]J. S. Geiger, R. L. Graham, I. Bergstrom, and F. Brown, Nucl. Phys. 68, 352 (1965).
[48]J. R. Van Hise, G. Chilosi, and N. J. Stone, Phys. Rev. 161, 1254 (1967).
[49]R. L. Bunting, Nucl. Data Sheets 15, 335 (1975).
[50]L. R. Greenwood, Nucl. Data Sheets 12, 139 (1974).
[51]G. Berzins, M. E. Bunker, and J. W. Starner, Nucl. Phys. A128, 294 (1969).
[52]A. de-Shalit, Phys. Rev. 122, 1530 (1961).
[53]V. Paar, Nucl. Phys. A211, 24 (1973).
[54]R. Almar, O. Civitorese, and F. Krmpotic, Phys. Rev. C 8, 1518 (1973).
[55]D. C. Choudhury and J. N. Friedman, Phys. Rev. C 3, 1619 (1971).
[56]A. Kuriyama, T. Marumori, and K. Matsuyanagi, Prog. Theoret. Phys. 45, 784 (1971).
[57]A. Kuriyama, T. Marumori, and K. Matsuyanagi, Prog. Theoret. Phys. 47, 489 (1972).
[58]A. Kuriyama, T. Marumori, and K. Matsuyanagi, Prog. Theoret. Phys. 51, 779 (1974).
[59]A. Kuriyama, T. Marumori, K. Matsuyanagi, and R. Okamoto, Prog. Theoret. Phys. 53, 489 (1975).
[60]H. Yukawa, Suppl. Prog. Theoret. Phys. No. 58 (1975).
[61]G. Alaga, Institute "Ruder Boskovic," 41001 Zagreb, Croatia, Yugoslovia, private communication.
[62]A. Faessler, Kernforschungsanlagt, Jülich GmbH, Institute für Kernphysik, D-5170, Jülich 1, Germany, private communication.
[63]S. V. Jackson, W. B. Walters, and R. A. Meyer, Phys. Rev. C 13, 808 (1976).
[64]K. Heyde, M. Waroquier, and R. A. Meyer, Phys. Rev. C 18, 1219 (1978).
[65]M. D. Glascock, W. B. Walters, and R. A. Meyer, Bull. Am. Phys. Soc. 21, 634 (1976).
[66]E. Schneider, W. B. Walters, and R. A. Meyer, Z. Phys. A283, 415 (1977).
[67]M. D. Glascock, E. W. Schneider, P. W. Gallagher, W. B. Walters, and R. A. Meyer, in Proceedings of the International Conference on Nuclear Structure (Tokyo, 1977) (unpublished), p. 346.
[68]H. Toki, Institute für Kernphysik, KFA Jülich, Germany, private communication.
[69]H. Toki and A. Faessler, A. Phys. A276, 35 (1976).